

High-resolution observations on fine-scale spatial and temporal heterogeneity of phytoplankton communities using FlowCAM

KHIN KHIN GYI¹⁾, Takuo OMURA^{2, 3)}*, Rie NAKAMURA³⁾ and Yuji TANAKA^{1, 2)}

Abstract: To understand the fine-scale spatio-temporal phytoplankton dynamics with reference to the environmental properties of the water column, high-frequency samplings every 4 h, at 0.5–2 m depth intervals using a submersible pump was conducted in Tateyama Bay, Japan, for 24 h from 12 h of 12 May to 08 h of 13 May 2017. The FlowCAM, which is an automatic device, was used to identify, count and size the phytoplankton. As a result, the phytoplankton distribution significantly varied within a few meters and a short timescale (several hours) of a day. For example, *Thalassiosira* sp. and *Prorocentrum minimum* were detected at all sampling depths and times rather evenly, but the water-column total abundance of *Dactyliosolen fragilissimus* and *Scrippsiella trochoidea* significantly decreased after the 2nd set of the samplings. Species-specific vertical distributions were various but related to the condition (strength and depth) of the thermocline at each sampling time. These phytoplankton species-specific distributions and variations in the composition reflect the eco-physiological characteristics and size structure of phytoplankton and the short-term hydrodynamic events. The high value of chlorophyll-*a* in the bottom layers was not only from the phytoplankton but also from the fluorescence of the aggregate particles.

Keywords : *phytoplankton, spatio-temporal distribution, FlowCAM, fine-scale sampling*

1) Graduate School of Marine Science and Technology, Tokyo University of Marine Science and Technology, 4-5-7 Konan, Minato, Tokyo 108-8477, Japan

2) Department of Ocean Sciences, School of Marine Resources and Environment, Tokyo University of Marine Science and Technology, 4-5-7 Konan, Minato, Tokyo 108-8477, Japan

3) Laboratory of Aquatic Science Consultant, 2-30-17 Higashikamata, Ota, Tokyo 144-0031, Japan

*Corresponding author: Takuo OMURA

Tel: 03-6428-6715

Fax: 03-6428-6716

E-mail: omura@lasc.co.jp

1. Introduction

The vertical distribution of phytoplankton community in the water column is highly heterogeneous in response to the small-scale physical hydrodynamic changes such as water mass stability (MELLARD *et al.*, 2011), vertical mixing (MAZNAH *et al.*, 2016), and the availability of light (TILZER and GOLDMAN, 1978). Variations of the abiotic water conditions occur naturally at different timescales throughout the day (GAST *et al.*, 2014), related with the periodic oscillations of the tidal currents (BLAUW *et al.*, 2012), which in turn influence the short-term changes in the phytoplankton community.

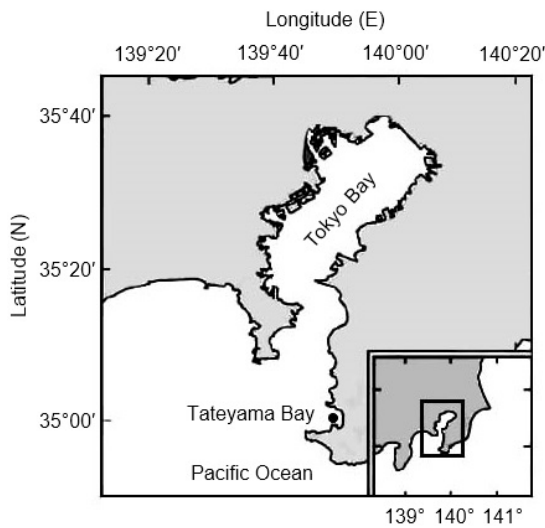


Fig. 1 The sampling site (solid circle) in Tateyama Bay, Japan.

Despite the relationship between environmental properties, ecological characteristics and fine-scale phytoplankton dynamics has been reported by previous studies (*e.g.* DEKSHENIEKS *et al.*, 2001; GERVAIS *et al.*, 2003; LUNVEN *et al.*, 2005; CARON *et al.*, 2008), it is still remaining to explore how do phytoplankton fluctuate throughout the entire water column, in a short timescale of the day. Hence, we here conducted a series of pump samplings throughout the whole vertical water column, at a relatively fine-scale of 0.5–2 m depth interval, every 4 h, dealing with the physical characteristics of the water column. The aim was to understand the precise spatial and temporal distributions of phytoplankton abundance, composition and the size structure, together with the particle distribution data, and thus provide relevant information about the short-term changes in the phytoplankton vertical distribution and the community dynamics. In the case of monitoring the high-resolution field survey data, traditional microscopic examination is time-consuming. To overcome this difficulty, we de-

ployed an automatic device FlowCAM (the Flow Cytometer And Microscope), which has combined capabilities of flow cytometry, microscopy and image analysis (SIERACKI *et al.*, 1998). This apparatus counts and photographs particles moving in a fluid flow. To create this flow, the water sample is drawn into the instrument by means of a peristaltic pump. A digital camera photographs the particles as they pass through a prismatic glass chamber mounted on a cell holder in front of a microscope lens (POULTON and MARTIN, 2010). The FlowCAM provides informative information for plankton study as follows: (1) cell counts and sizing accuracy (SIERACKI, *et al.*, 1998; SEE *et al.*, 2005; TAUXE *et al.*, 2006; ÁLVAREZ *et al.*, 2014), and (2) high-quality images for species identification as a VisualSpreadsheets (CAMOYING and YÑIGUEZ, 2016). Taking these advantages of FlowCAM, we can reduce the time for sample processing and increase the resolution of the field survey.

2. Materials and methods

2.1 Sampling site and sample collection

The sampling was carried out onboard a training ship *Seiyo-maru* of Tokyo University of Marine Science and Technology anchored at a point of 23 m deep in Tateyama Bay (35°00.06' N, 139°49.87' E), Japan (Fig. 1). On 12–13 May 2017, a total of six samplings were conducted every 4 h at 12, 16, 20, 00, 04 and 08 h (JST). Water samples were obtained using a vortex submersible pump (pumping speed: 0.5 m³ min⁻¹) following the method of ITOH *et al.* (2011), which is originally consulting the depth discrete pump sampling system shown in HARRIS *et al.* (1986). The depth interval was set every 0.5 m from 0 to 14 m, and 2 m from 16 to 20 m depth. We collected 192 samples in total, from 32 distinct vertical water layers within 0–20 m depth. For the phytoplankton analysis, water samples of 500 mL

were collected and immediately fixed with formalin (final concentration 1%). Concurrently, vertical profiles of water temperature, salinity, and density (σ_t) were taken using a CTD (AAQ-RINKO, JFE Advantech, Co., Ltd., Tokyo, Japan) fitted with an *in vivo* chlorophyll-*a* fluorescence sensor, a nephelometric sensor, and photosynthetically active radiation (PAR) sensor. At each time, a series of pump sampling was completed within about an hour.

Sunrise and sunset were at 04:39 and 18:34, on the sampling days. The first day (May 12) was calm and sunny while the second day (May 13) was quite windy and rainy. Information about the tide level of the sampling area was obtained from the Japan Meteorological Agency website (http://www.data.jma.go.jp/kaiyou/data/db/tide/suisan/pdf_hourly/2017/TT.pdf). Two low tides and two high tides were included during the sampling period (Fig. 2).

2.2 Phytoplankton and aggregate particle analyses by the FlowCAM

Phytoplankton samples were counted in triplicate using the automatic sample analysis device, FlowCAM (Fluid Imaging Technologies, Inc., ME, USA). In this study, particle images were captured by the FlowCAM auto-image mode, with an imaging rate of 5 frames per second, the FC100 flow cell (100 μm chamber depth) and the 10 x objective lens. The flow rate was controlled by the rotation rate of the pump (0.14 mL min^{-1}). Phytoplankton were identified by visual inspection using the image analysis software (VisualSpreadsheet: VSS) in FlowCAM system, and Equivalent Spherical Diameter (ESD) volume by the FlowCAM was used as a proxy for the estimation of phytoplankton biovolume. The ESD-based volume (V_{ESD}) is calculated based on the mean of 36 feret measurements which was conducted every 5° of specified directions

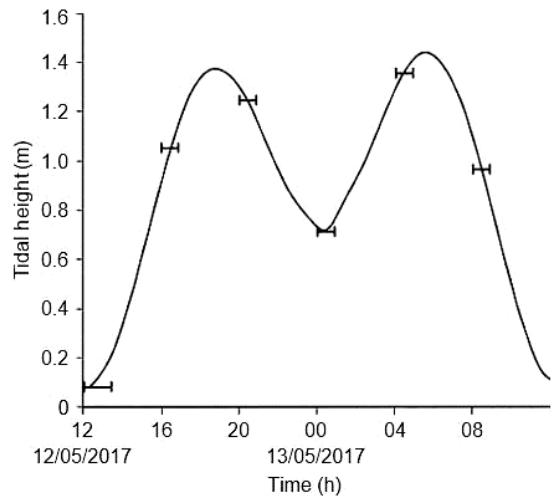


Fig. 2 Tide level (m) during the survey at Tateyama Bay, Japan. Bars represent start and end times of the samplings.

around the particle. Aggregate particles were checked and counted using VSS generated by the FlowCAM.

3. Results

3.1 Hydrological conditions (Figs. 3 and 4)

At 12 and 16 h, the upper layer (top 6 m) was heated by the solar radiation forming a certain gradient of water temperature (18.5–17.0 °C). The water column condition changed at 20 h, due to the intrusion of colder (15.5–13.5 °C) and saltier (34.4–34.6) water from the bottom during the flood. This intrusion mixed vertically the water column but was not strong enough to break the stratification up to the upper layer, forming a shallow layer thermocline at 1–6 m depth. At 00 h, when the water intrusion of the flood tide moved downward, and a thermocline was found at a deeper depth, 16–19 m with a temperature gradient (15.5–14.0 °C). At 04 h, the water column was well-mixed due to the high tidal current, and the colder and saltier water layer was located even deeper and almost not visible in our

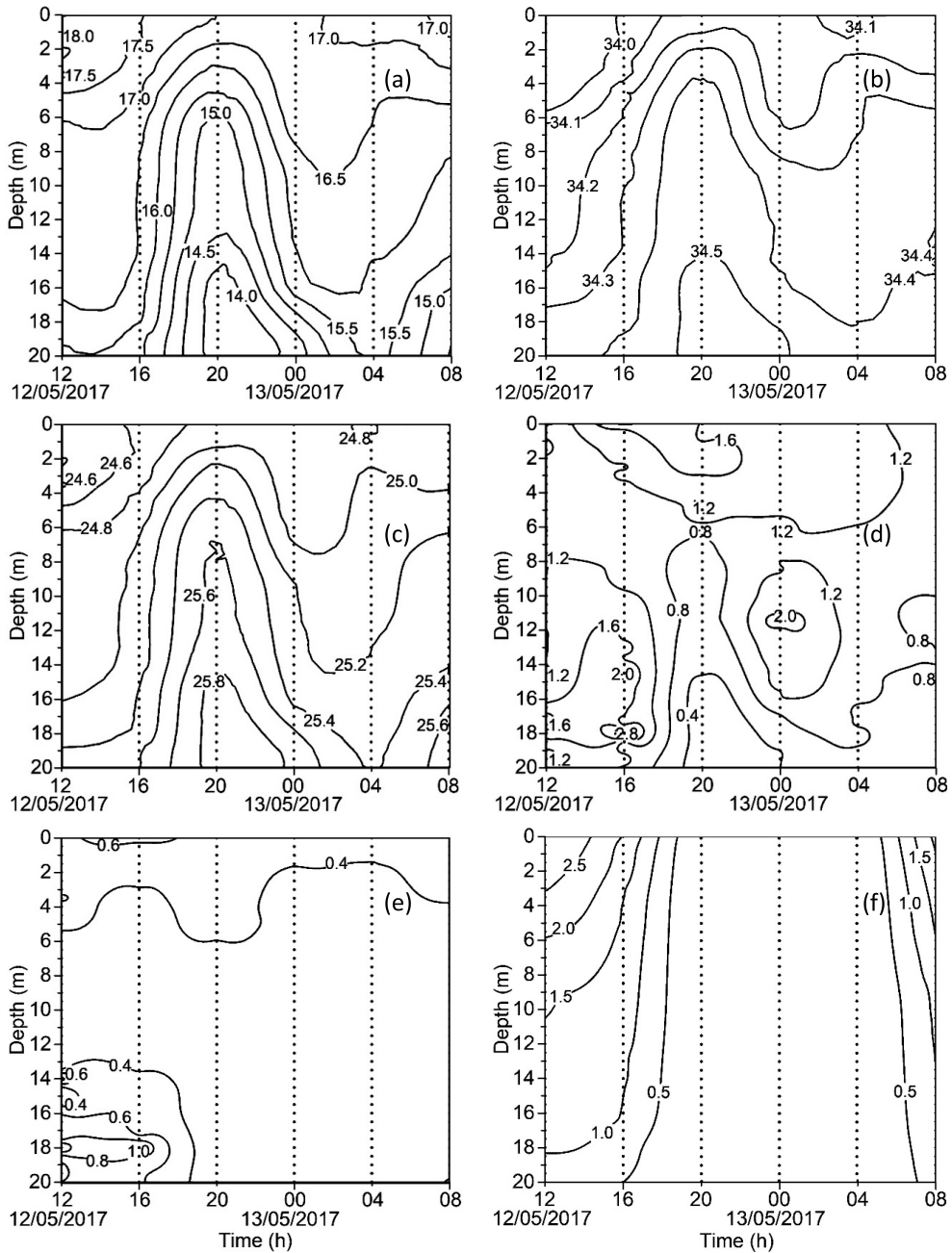


Fig. 3 Temporal changes in the vertical distribution of environmental properties on 12–13 May 2017. (a) water temperature ($^{\circ}\text{C}$), (b) salinity, (c) sigma- t , (d) Chl- a ($\mu\text{g L}^{-1}$), (e) turbidity (FTU), and (f) light intensity (PAR in $\log_{10} \mu\text{mol photons m}^{-2}\text{s}^{-1}$).

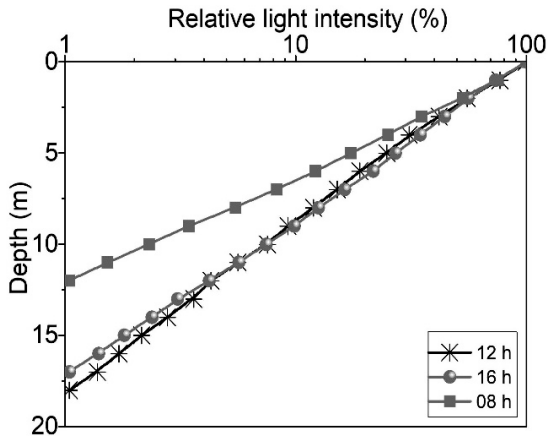


Fig. 4 Temporal changes in the vertical distribution of relative light intensity during 12–13 May 2017.

profiles. Later, at 08 h, the flood lifted this water mass again upwards, reaching the 16 m depth. At this time, the upper layer (0–14 m) remained well-mixed, showing a more homogeneous distribution of environmental parameters (Figs. 3a, b). The density profile showed the similar fluctuations governed by the temperature and salinity (Fig. 3c).

Regarding the chlorophyll-*a* fluorescence (Chl-*a*), the colder and saltier water found in the deeper layer that moved upwards during high tide showed distinctively low Chl-*a* (0.2–0.8 $\mu\text{g L}^{-1}$). Above this pool, typical peaks of Chl-*a* (1.6 and 3.1 $\mu\text{g L}^{-1}$) were observed at the bottom 18 m at 12 and 16 h, but at 20 h, peak (1.8 $\mu\text{g L}^{-1}$) moved to the upper layer 2.5 m, coincided with a thermocline, and then moved back to the deeper depth 11.5 m at 00 h, and disappeared in 04 and 08 h, respectively (Fig. 3d). Water turbidity was higher at 12 and 16 h, especially in the bottom layers where a significant increase in the Chl-*a* was noticed (Fig. 3e). The values of 1% I_0 depths (which indicate the bottom of the euphotic layer) in the day-time samplings were 18 m at 12 h, 17 m at 16 h and 12 m at 08 h, respec-

tively (Figs. 3f and 4).

3.2 Spatial and temporal distributions of total phytoplankton (Fig. 5)

At 12 h, phytoplankton distribution was heterogeneous with high densities 134 ± 13 cells mL^{-1} (mean \pm standard deviation) in the upper 0–4 m, and 115 ± 20 cells mL^{-1} at 7.5–20 m, respectively, and a low density 72 ± 26 cells mL^{-1} in the thermocline 4.5–7 m (Fig. 5a). At 16 h, phytoplankton showed a similar distribution pattern to that observed at 12 h, with high density 100 ± 13 cells mL^{-1} in the upper 4 m but decreased to 70 ± 9 cells mL^{-1} in the thermocline (4.5–7 m) and again an increasing trend 90 ± 19 cells mL^{-1} was observed below 7 m towards the bottom 20 m (Fig. 5b). Phytoplankton distribution pattern totally changed at 20 h, which was characterized by the formation of the pronounced thermocline at a shallow depth (1–6 m), where phytoplankton were concentrated 61 ± 21 cells mL^{-1} , but the distribution was restricted below the thermocline (Fig. 5c). At 00 h, thermal stratification in the upper layer was not seen, but it appeared in a deeper layer (16–19 m). At that time, phytoplankton were abundant (76 ± 11 cells mL^{-1}) above the thermocline at 9–14 m (Fig. 5d) and significantly decreased in the thermocline. The next samplings at 04 and 08 h, phytoplankton showed a rather homogeneous vertical distribution pattern in the water column (Figs. 5e, f), correspond with the effects of tidal mixing.

3.3 Phytoplankton assemblage composition (Table 1)

In our survey, a total of 22 phytoplankton taxa were identified, including 9 diatoms (Bacillariophyceae) such as *Thalassiosira* sp. (3,520 cells mL^{-1} , 27.5%), *Dactyliosolen fragilissimus* (1,776 cells mL^{-1} , 13.9%), *Pseudo-nitzschia* sp. (927

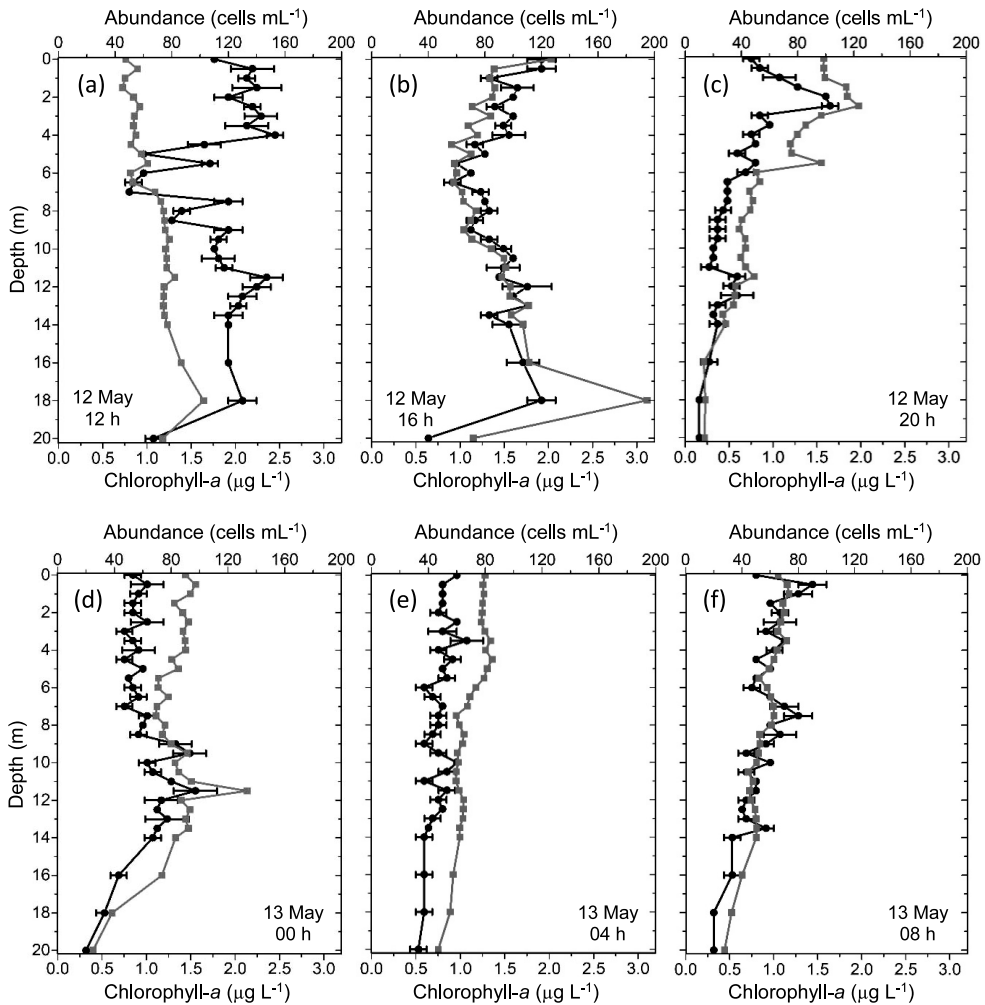


Fig. 5 Vertical distribution of total phytoplankton abundance for the six sampling times. Black line: average phytoplankton abundance, with standard deviation bar from the triplicate counts. Grey line: Chl-*a* concentration.

cells mL⁻¹, 7.2%), *Coscinodiscus* sp. (183 cells mL⁻¹, 1.4%), *Pleurosigma* sp. (49 cells mL⁻¹, 0.4%), *Lauderia annulata* (37 cells mL⁻¹, 0.3%), *Rhizosolenia setigera* (17 cells mL⁻¹, 0.1%), *Thalassionema nitzschioides* (13 cells mL⁻¹, 0.1%), and *Meuniera membranacea* (6 cells mL⁻¹, 0.05%); 10 dinoflagellates (Dinophyceae) such as *Prorocentrum minimum* (2, 622 cells mL⁻¹, 20.5%), *Scrippsiella trochoidea* (1,612 cells mL⁻¹,

12.6%), *Gyrodinium spirale* (501 cells mL⁻¹, 3.9%), *Protoperidinium quinquecorne* (253 cells mL⁻¹, 2.0%), *Heterocapsa* sp. (177 cells mL⁻¹, 1.4%), *Oxyphysis oxytoxoides* (76 cells mL⁻¹, 0.6%), *Ceratium furca* (23 cells mL⁻¹, 0.2%), *C. fusus* (7 cells mL⁻¹, 0.05%), *Gonyaulax spinifera* (10 cells mL⁻¹, 0.1%), and *Alexandrium* sp. (7 cells mL⁻¹, 0.05%); and other groups such as Raphidophyceae, Dictyochophyceae and Haptophy-

Table 1. List of phytoplankton in Tateyama Bay with total abundance, percentage, and average size (length and width).

Species	Total abundance		Length (μm)	Width (μm)
	cells mL^{-1}	%		
Bacillariophyceae				
<i>Coscinodiscus</i> sp.	183	1.4	50.0	37.7
<i>Dactyliosolen fragilissimus</i>	1,776	13.9	23.0	12.0
<i>Lauderia annulata</i>	37	0.3	23.7	16.9
<i>Meuniera membranacea</i>	6	0.05	57.8	31.1
<i>Pleurosigma</i> sp.	49	0.4	150.6	20.2
<i>Pseudo-nitzschia</i> sp.	927	7.2	30.3	4.6
<i>Rhizosolenia setigera</i>	17	0.1	379.0	5.2
<i>Thalassionema nitzschioides</i>	13	0.1	25.0	2.9
<i>Thalassiosira</i> sp.	3,520	27.5	18.9	12.5
Dinophyceae				
<i>Alexandrium</i> sp.	7	0.05	39.1	35.2
<i>Ceratium furca</i>	23	0.2	153.6	34.2
<i>Ceratium fusus</i>	7	0.05	343.7	30.5
<i>Gonyaulax spinifera</i>	10	0.1	29.6	23.1
<i>Gyrodinium spirale</i>	501	3.9	60.9	36.8
<i>Heterocapsa</i> sp.	177	1.4	30.7	21.1
<i>Oxyphysis oxytoxoides</i>	76	0.6	56.9	19.4
<i>Prorocentrum minimum</i>	2,622	20.5	22.2	18.5
<i>Protoperidinium quinquecorne</i>	253	2.0	23.7	18.7
<i>Scrippsiella trochoidea</i>	1,612	12.6	29.1	23.1
Dictyochophyceae				
<i>Dictyocha speculum</i>	10	0.1	29.5	21.3
Haptophyceae				
Coccolithophorid	468	3.7	13.2	12.3
Raphidophyceae				
<i>Heterosigma akashiwo</i>	303	2.4	29.8	24.3
Unidentified phytoplankton	205	1.5	13.9	11.9

ceae with only one species of each, *Heterosigma akashiwo* (303 cells mL^{-1} , 2.4%), *Dictyocha speculum* (10 cells mL^{-1} , 0.1%), and Coccolithophorid (468 cells mL^{-1} , 3.7%), respectively, and unidentified phytoplankton (205 cells mL^{-1} , 1.5%). Hence, the phytoplankton community was mainly dominated by diatoms and dinoflagellates (50%

and 42% of the total cell density).

Specifically, among these species, *Thalassiosira* sp., *D. fragilissimus*, *Pseudo-nitzschia* sp., *P. minimum*, and *S. trochoidea* were noted as the dominant species, which altogether contributed more than 80% of the total abundance of phytoplankton. Therefore, we consider their species-

specific distribution patterns in detail. The other species such as *L. annulata*, *Coscinodiscus* sp., *Rhizosolenia* sp., *T. nitzschioides*, *M. membranacea*, *Pleurosigma* sp., *G. spirale*, *Alexandrium* sp., *G. spinifera*, and *Heterocapsa* sp. were not observed in the colder and saltier water. Some dominant phytoplankton and the additional five species, *P. quinquecorne*, *O. oxytoxoides*, *C. furca*, *C. fusus*, and *D. speculum* that appeared after the high tide, only occurred in the colder and saltier water.

3.4 Species-specific distributions of dominant phytoplankton species (Fig. 6)

Thalassiosira sp. was numerically dominant throughout the study period and found at all sampling depths and times (Fig. 6a). *D. fragilissimus* distribution coincided with the thermocline, and they were trapped in the thermocline (1–6 m) at 20 h by the strong density gradients. Moreover, the cell density decreased to approximately the half (50%) after the high tide (18:20) and was not observed in the colder and saltier water mass (Fig. 6b). *Pseudo-nitzschia* sp. distribution pattern was not clear due to its low cell density throughout the sampling period (Fig. 6c). Similarly to *Thalassiosira* sp., *P. minimum* was detected at all sampling depths and times. An exception occurred at 20 h when a strong thermocline was marked at 1–6 m depth, where high cell densities were observed, but the distribution was limited below the thermocline (Fig. 6d). *S. trochoidea* distributed mainly in the first two samplings at 12 and 16 h; however, its distribution completely changed, and the abundance decreased to three-fourths (75%) after the high tide, 18:20 (Fig. 6e).

3.5 Phytoplankton biovolume versus Chl-*a* (Fig. 7)

At 12 and 16 h, the slope of the regression line

showed a negative correlation ($p > 0.05$), and an inverse relationship between the Chl-*a* and phytoplankton biovolume was observed (Figs. 7a, b). Thus, relatively low phytoplankton biovolume was found at a depth of Chl-*a* peak 18 m, where small-sized diatom, *Thalassiosira* sp. (Table 1) was dominant in those samples. At 20 h, a statistically positive correlation ($p < 0.05$) was seen between the Chl-*a* and biovolume. At that time, Chl-*a* peak occurred in the upper layer (1–6 m), where higher phytoplankton biovolume was observed (Fig. 7c). In the following sample at 00 h, Chl-*a* and biovolume showed a positive correlation due to the occurrence of large-sized dinoflagellates above the thermocline (9–14 m) where the Chl-*a* peak was detected (Fig. 7d). A positive relationship was detected between the Chl-*a* and biovolume for 04 and 08 h, respectively (Figs. 7e, f).

An allometric relationship of Chl-*a* with biovolume was found in most sampling times except for 12 and 16 h. At these times, the Chl-*a* peak was observed at the bottom layer where higher turbidity was recorded.

3.6 Vertical distribution of aggregate particles (Fig. 8)

Aggregates were generally more abundant in the first two samplings at 12 and 16 h (before high tide), especially at the bottom layers, with higher turbidity. After high tide (18:20), the formation of high abundance was not observed at the bottom in the following samplings at 20, 00, 04 and 08 h.

4. Discussion

Short-term phytoplankton dynamics are related to the changes of the water masses and hydrodynamic gradients such as stratification and mixing processes, influenced by the periodic oscillations of the tidal currents (BLAUW *et al.*,

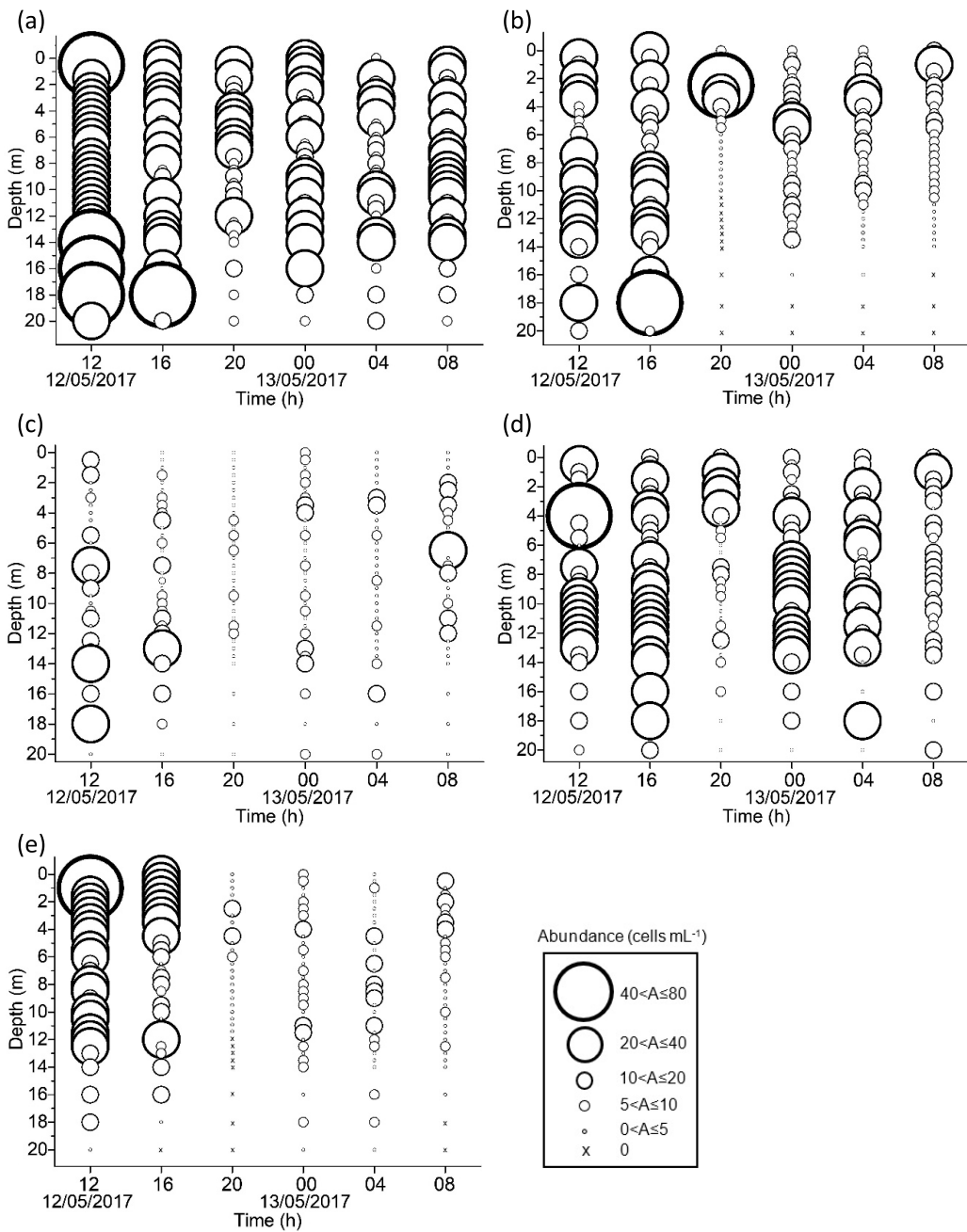


Fig. 6 Vertical distribution of dominant phytoplankton species (average of the six samplings): (a) *Thalassiosira* sp., (b) *Dactyliosolen fragilissimus*, (c) *Pseudo-nitzschia* sp., (d) *Prorocentrum minimum*, and (e) *Scrippsiella trochoidea*. “A” in the explanatory box represents “Abundance.”

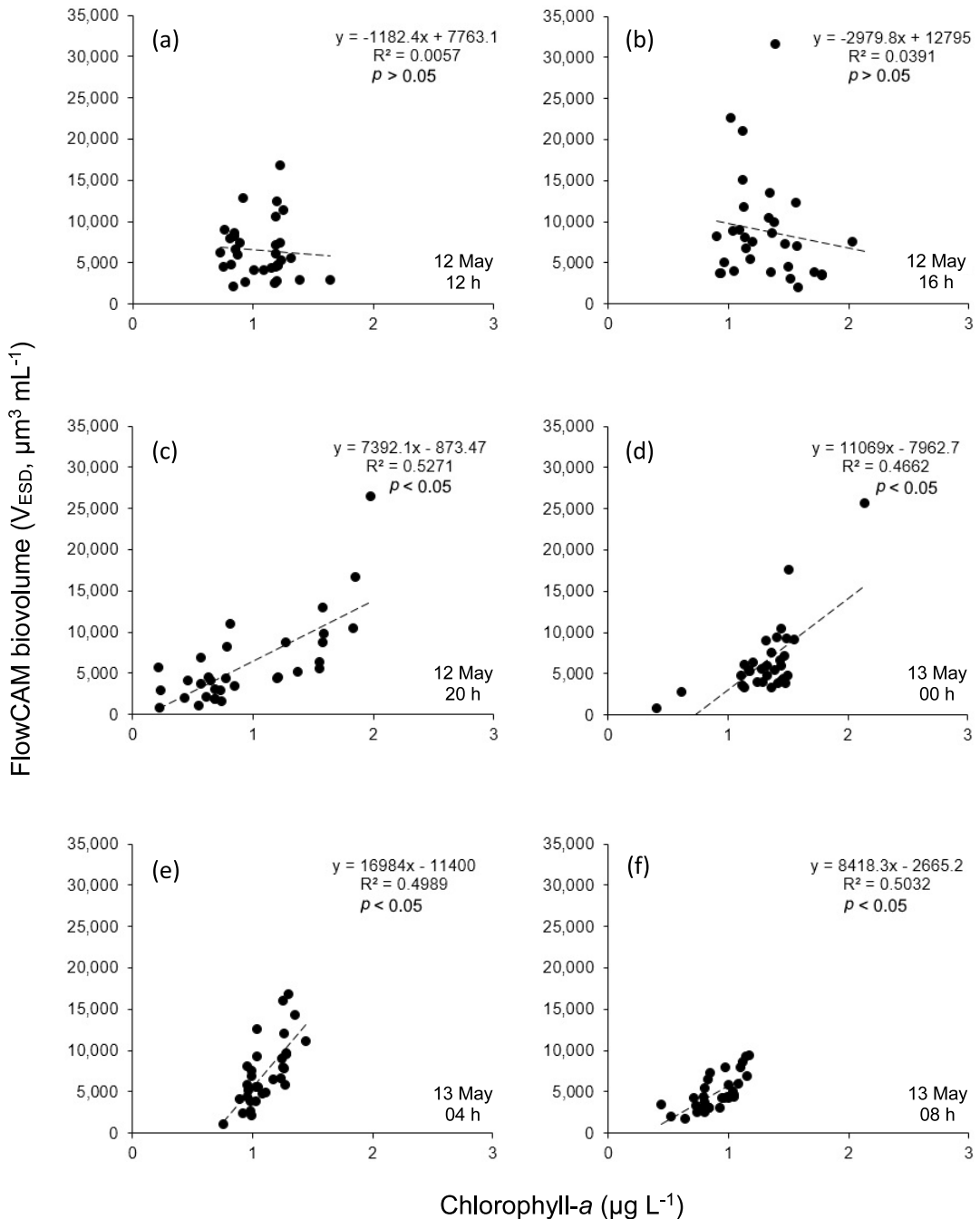


Fig. 7 Relationship between Chl-*a* and FlowCAM biovolume of total phytoplankton from the cell counts for 32 distinct vertical water layers ($n = 32$) during six sampling times. (a), (b), and (c) are for 12h, 16h, and 20h of 12 May; (d), (e), and (f) for 00h, 04h, and 08h of 13 May, respectively. The dashed line is fitted regression line.

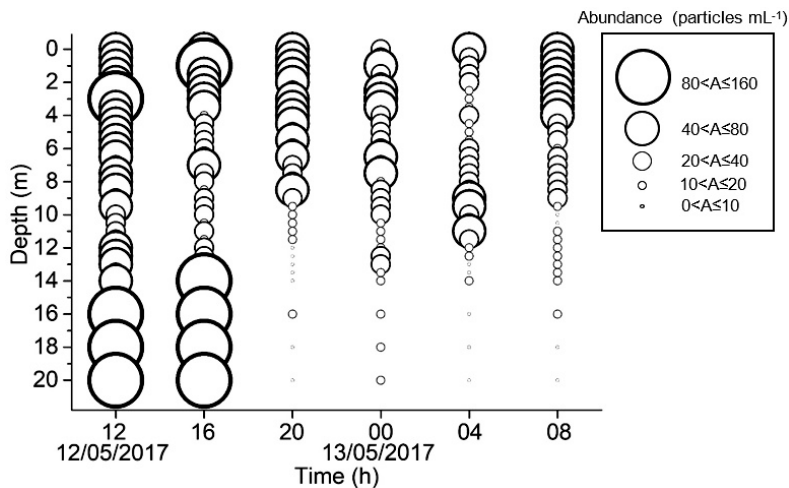


Fig. 8 Vertical distribution of aggregate abundance (average value of the triplicate analysis) for six sampling times. “A” in the explanatory box represents “Abundance.”

2012). During our study period, thermal stratification was likely to be influencing the spatial heterogeneity of phytoplankton distribution. Stratification was pronounced under weak tidal mixing condition. Temperature gradients then divided the water column into different strata by the density gradients that restricted the phytoplankton (but not entirely inhibit), resulting in a heterogeneous distribution. In contrast, it is likely that the vertical mixing generated by the tidal current homogenized the phytoplankton distribution in the water column. However, if tidal mixing was not strong enough, the water column could not be fully mixed, and stratification would remain in the upper layer. Thus, phytoplankton and Chl-*a* distributions differed among depths and sampling times due to the changes of the water masses and thermal structure.

In our study, both diatoms and dinoflagellates dominated the phytoplankton community. However, their composition to the phytoplankton community was different in the different layers and times, related with the changes of the water

mass structure, and probably the thickness of the euphotic layer. Changes were pronounced in the day-time at 12 and 16 h, when stratification of water mass force to form the diatoms and dinoflagellates aggregation in the water column. At these times, a large proportion of diatoms contributed to the phytoplankton community near the bottom where a high value of Chl-*a* was observed (Fig. 9a). In contrast, dinoflagellates were detected mainly in the upper water column coinciding with the thermocline but rarely observed in the deeper parts of the euphotic zone (Fig. 9b). This might be because the dinoflagellates prefer stratified water mass as has been explained in classical literatures (*e.g.* SMAYDA and REYNOLDS, 2001).

Thalassiosira sp. and *P. minimum* occurred at all sampling depths and times. These are euryhaline and eurythermal species, that are common in temperate coastal environments (POPOVICH and GAYOSO, 1999; HAJDU *et al.*, 2005). However, *D. fragilissimus* and *S. trochoidea* significantly decreased their abundance after the high tide,

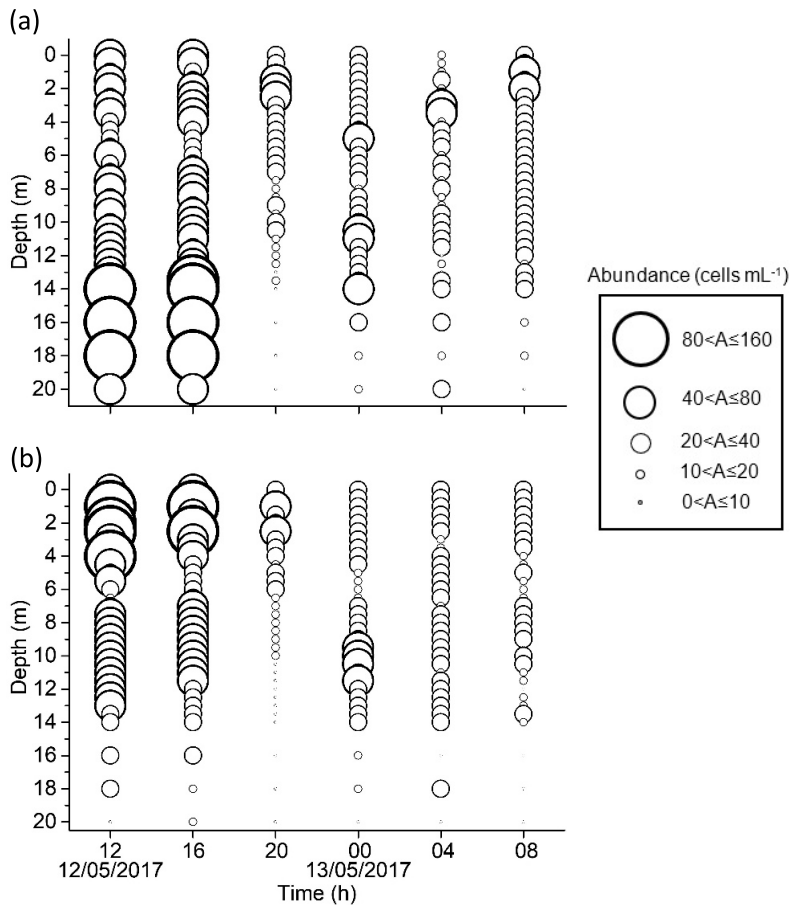


Fig. 9 Vertical distribution of (a): diatoms and (b): dinoflagellates abundance (average value of the triplicate analysis) for six sampling times. “A” in the explanatory box represents “Abundance.”

perhaps due to the changes of the water mass. During our survey, most phytoplankton species suddenly disappeared (except some dominant phytoplankton) after the high tide, when colder and saltier water mass intruded. It is suggested that these clear changes in species composition probably related to the changes of the water mass. Additionally, only five phytoplankton species, *P. quinquecorne*, *O. oxytoxoides*, *C. furca*, *C. fusus*, and *D. speculum* occurred in the colder and saltier water. Some of these five species (*C. furca* and *C. fusus*: Type VI (Coastal Entrained

Taxa)) were noted as the coastal habitat (SMAYDA and REYNOLDS, 2001).

Regarding the phytoplankton biovolume and Chl-*a*, a significant positive correlation was found in most sampling times except for 12 and 16 h. At these exceptional times, discrepancies were apparent because of the relatively low phytoplankton biovolume at a depth of Chl-*a* peak. In the case of 12 and 16 h, the water column was marked with a thermocline at 4.5–7 m depth, which may act as a barrier (SPRINTALL and CRONIN, 2001) between the upper and lower lay-

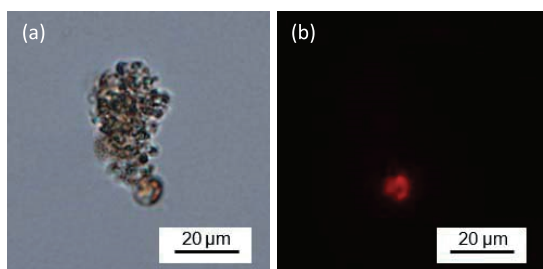


Fig. 10 Images of aggregates captured by an epi-fluorescence microscope using a fresh bottom sample obtained from Tokyo Bay as a trial. (a): bright field of aggregates, (b): fluorescence emits from aggregate under the dark field.

er. In the present study, the phytoplankton community in the lower layer was dominated by the smaller size phytoplankton species, such as *Thalassiosira* sp. and *D. fragilissimus*. Thus, phytoplankton biovolume was higher in the upper layer than those at a depth of Chl-*a* peak. Hence, a question rises “why Chl-*a* was high near the bottom?” We here speculate that the turbidity may be the key to answer this question because higher turbidity values coincided with the bottom Chl-*a* peaks. MATSUIKE *et al.* (1986) reported the increase of suspended particles in the water column is the major cause of water turbidity. This condition of high particle concentration leads to promote particle aggregation by colliding of smaller particles (JACKSON, 1990) or the release of phytoplankton structural bodies (ARMBRECHT *et al.*, 2004), or together with sediments, and detritus (ZIMMERMANN-TIMM, 2002).

Our vertical profile of the aggregates showed that the particle densities were higher in the bottom at 12 and 16 h, where the highly turbid water mass was observed. However, it was gone after the high tide, probably due to the intrusion of low turbidity water. At the same time, the Chl-*a* peak at the bottom disappeared, suggesting the relationship between the Chl-*a* and aggregate

particles. Hence, an additional experiment was done for the fluorescence analysis of the aggregates. Unfortunately, our formalin-fixed samples could not be used in the experiment, and thus we collected the fresh samples from the bottom water of Tokyo Bay while plankton survey cruising at the inner Tokyo Bay. From our observation with an epi-fluorescence microscope, emission of fluorescence was detected from the aggregates (Figs. 10a, b). This finding provides additional evidence for the consideration of Chl-*a* concentration in Tateyama Bay, which shows the high value at the bottom is not only from the phytoplankton but also from the fluorescence due to the pigments deposited in the aggregate particles that were floating there.

5. Conclusions

To assess the fine-scale spatio-temporal phytoplankton dynamics over a short time period, we used FlowCAM which can rapidly count, identify and size the phytoplankton. Our results indicated that phytoplankton distribution changed significantly in a short timescale (such as several hours) and in a few meters in depths, related with the eco-physiological characteristics of phytoplankton, the stratification and vertical mixing. Therefore, studies based on monthly or seasonal survey of phytoplankton with depth-averaged samplings may not well reveal the real community structure and the distribution patterns of phytoplankton that vary within a short time. Furthermore, our results showed that “Chl-*a*” does not always represent the phytoplankton abundance because it can be affected by detrital aggregate particles that contain a significant amount of fluorescent substances.

Acknowledgments

We thank the Laboratory of Aquatic Science Consultant Co., Ltd., which provided the use of a

FlowCAM and lab facilities. Sincere thanks are to the captain and crew members of T/R/V Seiyo-maru and students of Plankton Laboratory of Tokyo University of Marine Science and Technology, who helped the field sampling of significant difficulties. The present work was partially supported by the Monbukagakusho Scholarship for KKG., and also by JSPS KAKENHI Grant Numbers JP18H02263 for YT.

References

- ÁLVAREZ, E., M. MOYANO, Á. LÓPEZ-URRUTIA, E. NOGUEIRA and R. SCHAREK (2014): Routine determination of plankton community composition and size structure: a comparison between FlowCAM and light microscopy. *J. Plankton Res.*, **36**, 170–184.
- ARMBRECHT, L. H., V. SMETACEK, P. ASSMY and C. KLAAS (2004): Cell death and aggregate formation in the giant diatom *Coscinodiscus wailesii* (Gran & Angst, 1931). *J. Exp. Mar. Biol. Ecol.*, **452**, 31–39.
- BLAUW, A. N., E. BENINCÀ, R. W. P. M. LAANE, N. GREENWOOD and J. HUISMAN (2012): Dancing with the tides: fluctuations of coastal phytoplankton orchestrated by different oscillatory modes of the tidal cycle. *PLoS ONE*, **7**, e49319–e49319.
- CAMOYING, M. G. and A. T. YÑIGUEZ (2016): FlowCAM optimization: Attaining good quality images for higher taxonomic classification resolution of natural phytoplankton samples. *Limnol. Oceanogr.: Methods*, **14**, 305–314.
- CARON, D. A., B. STAUFFER, S. MOORTHI, A. SINGH, M. BATALIN, E. A. GRAHAM, M. HANSEN, W. J. KAISER, J. DAS, A. PEREIRA, A. DHARIWAL, B. ZHANG, C. OBERG and G. S. SUKHATME (2008): Macro-to fine-scale spatial and temporal distributions and dynamics of phytoplankton and their environmental driving forces in a small montane lake in southern California, USA *Limnol. Oceanogr.*, **53**, 2333–2349.
- DEKSHENIEKS, M. M., P. L. DONAGHAY, J. M. SULLIVAN, J. E. B. RINES, T. R. OSBORN and M. S. TWARDOWSKI (2001): Temporal and spatial occurrence of thin phytoplankton layers in relation to physical processes. *Mar. Ecol. Prog. Ser.*, **223**, 61–71.
- GAST, L., A. N. MOURA, M. C. P. VILAR, M. K. CORDEIRO-ARAÚJO and M. C. BITTENCOURT-OLIVEIRA (2014): Vertical and temporal variation in phytoplankton assemblages correlated with environmental conditions in the Mundaú reservoir, semi-arid northeastern Brazil. *Braz. J. Biol.*, **74**, 93–102.
- GERVAIS, F., U. SIEDEL, B. HEILMANN, G. WEITHOFF, G. HEISIG-GUNKEL and A. NICKLISCH (2003): Small-scale vertical distribution of phytoplankton, nutrients and sulphide below the oxycline of a mesotrophic lake. *J. Plankton Res.*, **25**, 273–278.
- HAJDU, S., S. PERTOLA and H. KUOSA (2005): *Prorocentrum minimum* (Dinophyceae) in the Baltic Sea: morphology, occurrence- a review. *Harmful Algae*, **4**, 471–480.
- HARRIS, R. P., L. FORTIER and R. K. YOUNG (1986): A large-volume pump system for studies of the vertical distribution of fish larvae under open sea conditions. *J. Mar. Biol. Ass. U. K.*, **66**, 845–854.
- ITOH, H., A. TACHIBANA, H. NOMURA, Y. TANAKA, T. FUROTA and T. ISHIMARU (2011): Vertical distribution of planktonic copepods in Tokyo Bay in summer. *Plankton Benthos Res.*, **6**, 129–134.
- JACKSON, G. A. (1990): A model of the formation of marine algal flocs by physical coagulation processes. *Deep-Sea Res.*, **37**, 1197–1211.
- JAPAN METEOROLOGICAL AGENCY WEBSITE (2017): http://www.data.jma.go.jp/kaiyou/data/db/tide/suisan/pdf_hourly/2017/TT.pdf.
- LUNVEN, M., J. F. GUILLAUD, A. YOUÉNOU, M. P. CRASSOUS, R. BERRIC, E. LE GALL, R. KÉROUEL, C. LABRY and A. AMINOT (2005): Nutrient and phytoplankton distribution in the Loire River plume (Bay of Biscay, France) resolved by a new Fine Scale Sampler. *Estuar. Coast. Shelf Sci.*, **65**, 94–108.
- MATSUIKE, K., T. MORINAGA and T. HIRAOKA (1986): Turbidity distributions in Tokyo Bay and movement of the turbid water. *J. Tokyo Univ. Fish.*, **73**, 97–114.
- MAZNAH, W. O. W., S. RAHMAH, C. C. LIM, W. P. LEE, K. FATEMA and M. M. ISA (2016): Effects of tidal events on the composition and distribution of

- phytoplankton in Merbok river estuary Kedah, Malaysia. *Trop. Ecol.*, **57**, 213-229.
- MELLARD, J. P., K. YOSHIYAMA, E. LITCHMAN and C. A. KLAUSMEIER (2011): The vertical distribution of phytoplankton in stratified water columns. *J. Theor. Biol.*, **269**, 16-30.
- POPOVICH, C. A. and A. M. GAYOSO (1999): Effect of irradiance and temperature on the growth rate of *Thalassiosira curviseriata* Takano (Bacillariophyceae), a bloom diatom in Bahía Blanca estuary (Argentina). *J. Plankton Res.*, **21**, 1101-1110.
- POULTON, N. J. and J. L. MARTIN (2010): Imaging flow cytometry for quantitative phytoplankton analysis - FlowCAM. *In* Microscopic and Molecular Methods for Quantitative Phytoplankton Analysis. KARLSON, B., C. CUSACK and E. BRESNAN (eds.), UNESCO (IOC Manuals and Guides, no. 55.), Paris, p. 47-54.
- SEE, J. H., L. CAMPBELL, T. L. RICHARDSON, J. L. PINCKNEY and R. SHEN (2005): Combining new technologies for determination of phytoplankton community structure in the northern Gulf of Mexico. *J. Phycol.*, **41**, 305-310.
- SIERACKI, C. K., M. E. SIERACKI and C. S. YENTSCH (1998): An imaging in-flow system for automated analysis of marine microplankton. *Mar. Ecol. Prog. Ser.*, **168**, 285-296.
- SMAYDA, T. J. and C. S. REYNOLDS (2001): Community assembly in marine phytoplankton: application of recent models to harmful dinoflagellate blooms. *J. Plankton Res.*, **23**, 447-461.
- SPRINTALL, J. and M. F. CRONIN (2001): Upper ocean vertical structure. *In* Encyclopedia of Ocean Science. STEELE, J. H., S. A. THORPE and K. K. TUREKIAN (eds.), Academic Press, San Diego, p. 3120-3129.
- TAUXE, L., J. L. STEINDORF and A. HARRIS (2006): Depositional remanent magnetization: Toward an improved theoretical and experimental foundation. *Earth Planet. Sci. Lett.*, **244**, 515-529.
- TILZER, M. M. and C. R. GOLDMAN (1978): Importance of mixing, thermal stratification and light adaptation for phytoplankton in Lake Tahoe (California, Nevada). *Ecology*, **59**, 810-821.
- ZIMMERMANN-TIMM, H. (2002): Characteristics, dynamics and importance of aggregates in rivers - An invited review. *Int. Rev. Hydrobiol.*, **87**, 197-240.

Received: 26 April, 2019

Accepted: 6 August, 2019

Morphological changes in silvering stages of *Anguilla bicolor bicolor* collected from Segara Anakan, Central Java, Indonesia

Nur Indah SEPTRIANI¹⁾, Chinthaka Anushka HEWAVITHARANE¹⁾,
Bambang RETNOAJI²⁾ and Noritaka MOCHIOKA¹⁾*

Abstract: To understand the morphological changes during the silvering stages of *Anguilla bicolor bicolor*, 68 males and 39 females were collected from Segara Anakan in Cilacap, Central Java, Indonesia during December 2015 - September 2016, May 2017 and June 2018. Specimens were categorized into 5 stages based on body and pectoral fin coloration: Y1, Y2, S1, S2 and S3. Total length of silver males ranged from 342 mm to 501 mm, with mean \pm SD 414.83 ± 40.38 mm and were notably smaller than silver females which ranged from 674 mm to 937 mm (786.11 ± 68.98 mm). Silver females were present in catches throughout the year, with peak collection during the dry months (May and June). This corresponded to the only period when silver males were caught. Locomotion indices such as, tail, dorsal fin, anal fin, pectoral fin and eye increased with progression in silvering stages, while feeding behavior indices such as, both upper and lower jaw in males showed increasing, lower lip depth in females showed decreasing and upper lip depth in females showed decreasing and snout remained constant. The increase in locomotion indices suggested that *A. bicolor bicolor* from Segara Anakan underwent morphological changes in preparation for spawning migration similar to those of temperate species, but increasing upper and lower jaw in males together with all samples caught using baited traps, suggested that these tropical eels remained as feeding individuals even at late stage silver eels.

Keywords : *Anguilla bicolor bicolor*, silvering, morphological change, Segara Anakan

1. Introduction

The life cycle of anguillid eels is divided into 5 principle stages which are leptocephalus larvae,

1) Faculty of Agriculture, Kyushu University, 744 Motooka, Nishi-ku, Fukuoka, 819-0395, Japan

2) Faculty of Biology, Universitas Gadjah Mada, Jl. Teknika Selatan, Sinduadi, Mlati, Sleman, D.I. Yogyakarta, 55281, Indonesia

*Corresponding author:

Tel: + 81-92-802-4603

Fax: + 81-92-802-4603

E-mail: mochioka@agr.kyushu-u.ac.jp

glass eel, elver, yellow eel and silver eel stages (BERTIN, 1956). Leptocephalus larvae of tropical eel *Anguilla bicolor bicolor* migrate passively and drift following ocean currents in the eastern Indian Ocean (AOYAMA *et al.*, 2007). They then metamorphose into glass eels at continental shelves and enter coastal waters and actively migrate into estuaries and rivers (TESCH, 1980). Glass eels then become elvers which are distinguished through morphological and behavioral changes such as shortening of body length, deposition of guanine in intra-abdominal membrane

and a benthic migration (TESCH, 2003; FUKUDA *et al.*, 2013). The growth phase in their areas of distribution is termed the yellow eel stage where they may spend many years until they reach sexual maturity and develop into migrating silver eels. The silver stage eels display changes in body coloration which are due to physiological and environmental conditions (TESCH, 2003; DURIF *et al.*, 2005; HAGIHARA *et al.*, 2012). Metamorphosis of yellow eels to silver eels is difficult to distinguish and therefore, identifying silver eels which are on the verge of migration is determined through skin color (DURIF *et al.*, 2005).

OKAMURA *et al.* (2007) described the silvering stages for *A. japonica* using two characteristics which were the coloration of the ventral skin and pectoral fins. In this description, eels were divided into two yellow eel stages Y1 and Y2 and two silver eel stages S1 and S2. Y1, an early yellow eel stage was described as yellow eels without metallic hue at the base of pectoral fins, while Y2 was late stage yellow eels and described as having a metallic hue at the base of pectoral fins and without melanization at the tip of pectoral fins. S1 was early stage silver eels with complete melanization at the tip of pectoral fins but without a fully pigmented belly usually with a black or dark brown coloration while, S2 was late stage silver eels with black or dark brown coloration on the belly.

Further studies on the morphological changes during the silvering/migration process of *A. australis* in the Makara Stream, Lake Onoke, and Lake Ellesmere in New Zealand showed that migrant eels had dorsally flattened heads and the snout had a slightly chiseled appearance. Furthermore, lips had thinned and the pectoral fins were slightly elongated with a black fringe. Dorsally the skin was black/brown, bronze, or green with a lateral metallic bronze coloration. Coloration on the ventral surface was generally metal-

lic silver while the belly was bright silver (TODD, 1981).

Several other studies also focused on the morphological and physiological changes within the silvering process of anguillid eels. These included the changes of skin color and enlargement of eyes in *A. australis*, *A. dieffenbachii*, *A. anguilla*, *A. japonica*, *A. marmorata* and *A. celebesensis* (TODD 1981; DURIF *et al.*, 2005; OKAMURA *et al.*, 2007; HAGIHARA *et al.*, 2012), lengthening of pectoral fins in *A. anguilla* (DURIF *et al.*, 2005), degeneration of the gut in *A. anguilla* and *A. japonica* (DURIF *et al.*, 2005; OKAMURA *et al.*, 2007), increase of retinal sensitivity in *A. anguilla* (BOWMAKER *et al.*, 2008), changes of fat contents in *A. rostrata* and *A. anguilla* (LARSSON *et al.*, 1990; SVEDANG and WICKSTROM 1997), increase of fatty acid contents in the skeletal muscles in *A. anguilla* (EGGINTON 1986), and modification of swim bladder in rete mirabile, gas gland and submucosa in *A. japonica* (YAMADA *et al.*, 2001).

Although there have been several studies on the silvering processes of anguillid eels, majority of these have been on temperate species, while information on tropical eels are still lagging. Considering that 13 species/sub-species of the 19 anguillids currently known are determined to be tropical species with nine species found around Indonesian waters (SUGEHA *et al.*, 2008), it is important to efficiently identify the various silvering stages of anguillid eels using relatively clear and simple characteristics to facilitate easy monitoring studies. Morphological changes of silvering eels in Indonesia was first studied by HAGIHARA *et al.* (2012), which was conducted in Central Sulawesi, Lake Poso and described the silvering stages of *A. marmorata* and *A. celebesensis*, but failed to provide information on *A. bicolor*. Therefore, the present study was aimed at assessing the morphological changes within the silvering process of female and male *A. bicolor*

bicolor from Segara Anakan, Indonesia.

2. Materials and methods

Fish catchment sampling location and species identification

A total of 107 specimens of *A. bicolor bicolor* were used in the present study. Specimens were identified through morphological characters as described by EGE (1939). As all specimens were morphologically identical, 8 specimens with mean, minimum and maximum morphological characters were further subjected to genetic identification using a partial sequence of mitochondrial DNA 16S rRNA region (MINEGISHI *et al.*, 2005; TAWA *et al.*, 2012). Genetic identification was conducted to discriminate *A. bicolor bicolor* and *A. bicolor pacifica* as morphological identification between these species has been considerably difficult. DNA sequences were submitted to DDBJ (DNA Data Bank Japan) under the accession numbers LC433757–LC433764. Specimens were stored at the Kyushu University Museum (KYUM-PI 5382–5389).

Specimens were obtained from fishermen who collected eels in the Segara Anakan in Cilacap, Central Java, Indonesia (Fig.1), during December 2015–September 2016, May 2017 and June 2018.

These fishermen employed traditional Indonesian baited traps 'wuwu' and fishing gear with hooks 'ureg-ureg', and 'opyok' together with crabs, earthworms and frogs as bait. 'Wuwu' baited traps used by the fishermen were set in the evening during 5–6 pm, and were then retrieved the next morning during 3–5 am. 'Ureg-ureg' was used in the day during ebb tide, while 'opyok' was used during the night with flood tides. Specimens collected for this study were only available if fishermen had retrieved eels the previous day. Therefore shortcomings such as quantifying the frequency and effort at which

fishermen collected eels is unknown.

Silvering stages and sex determination

The silvering stages were characterized based on the percentage cover of black coloration of pectoral fins and percentage cover of metallic hue at the base of pectoral fins measured along the anterioposterio axis of the pectoral fin. Black color coverage of pectoral fins = 100 (BPC/PFL^{-1}) where BPC is the length of black color coverage of pectoral fins and PFL is the pectoral fin length. Metallic hue at the base of pectoral fins = 100 (MBP/BPF^{-1}), where MBP is the length of metallic hue at base of pectoral fin and BPF is the length of base of pectoral fin along the anteriorposterior axis. The percentage cover of silver color and metallic hue on the belly of specimens = 100 (MBC/VL^{-1}), where MBC is silver color and metallic hue on belly and VL is the length from the lateral midline to the ventral line and was measured along the dorsoventral axis (Fig. 2). These external morphological color changes appear to be similar for tropical eels as with temperate eels such as *A. japonica* (OKAMURA *et al.*, 2007; HAGIHARA *et al.*, 2012) and therefore used as a criterion for differentiating silver eel stages in the present study. Sex was determined through visual inspection of external morphology. Specimens with lobed gonads were considered as males, described by BERTIN (1956), while specimens having gonads resembling frilled ribbons of tissue were considered as females as described by TODD (1981).

Morphological measurement

Specimens were transported to the laboratory and anaesthetized with 50 ppm Tricaine Methanesulfonate (MS222) before being examined and measured for morphological characteristics (Fig. 3) using a digital vernier caliper to the nearest 0.01 mm. Body weight of specimens were meas-

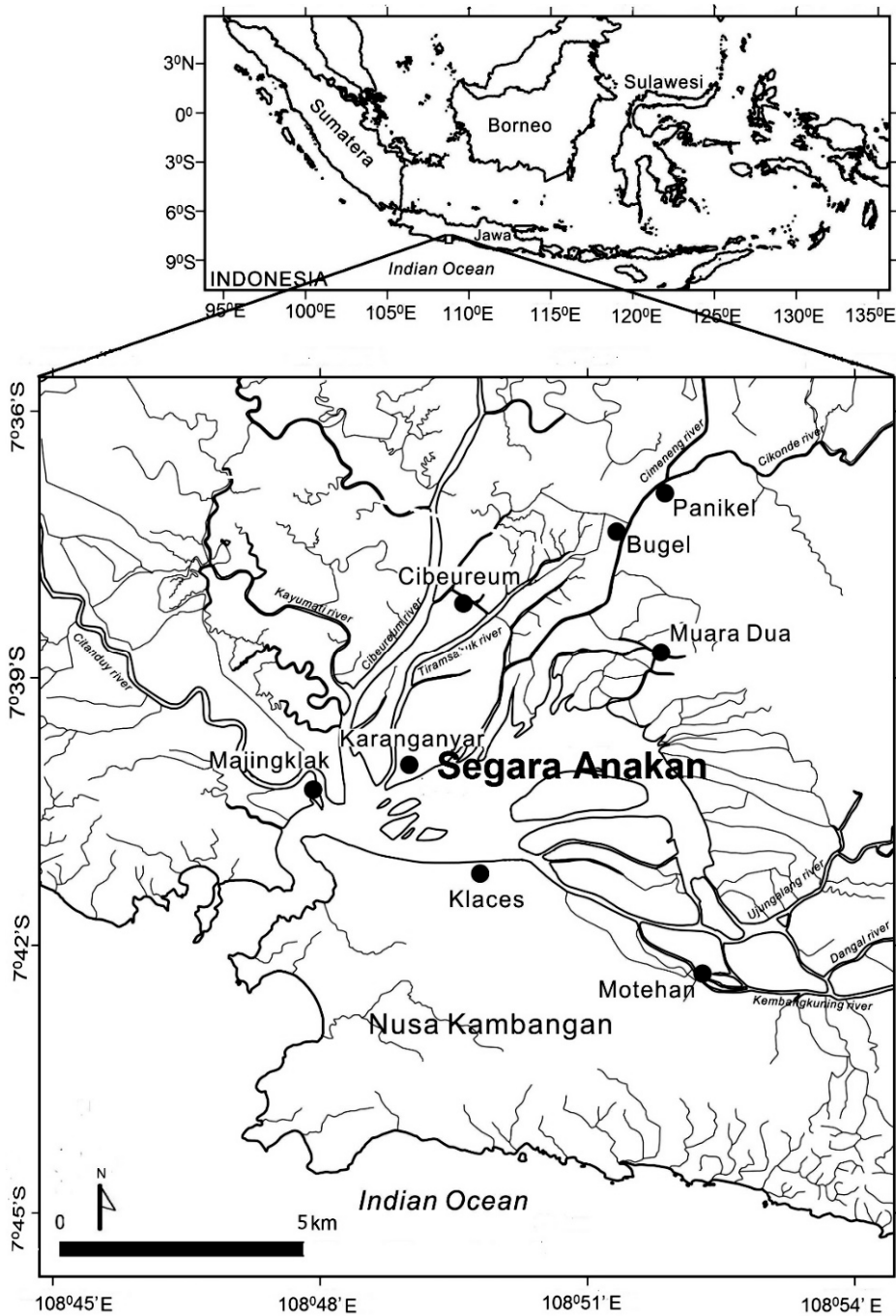


Fig. 1 Locations where *A. bicolor bicolor* were collected by fishermen. Map showing the location of Segara Anakan in Java Island, Indonesia near Indian Ocean.

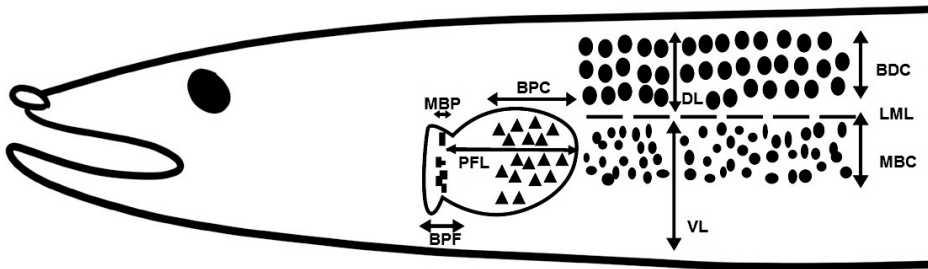


Fig. 2 Diagram showing measurements used for determining silvering stages of *A. bicolor bicolor* from Segara Anakan, Indonesia.

Base pectoral fin (BPF), black color coverage of pectoral fin (BPC:▲), black dorsal coloration (BDC:●), dorsal line (DL), lateral midline (LML), metallic belly coloration (MBC:●) (metallic hue at the base of pectoral fin (MBP:■), pectoral fin length (PFL), ventral line (VL)

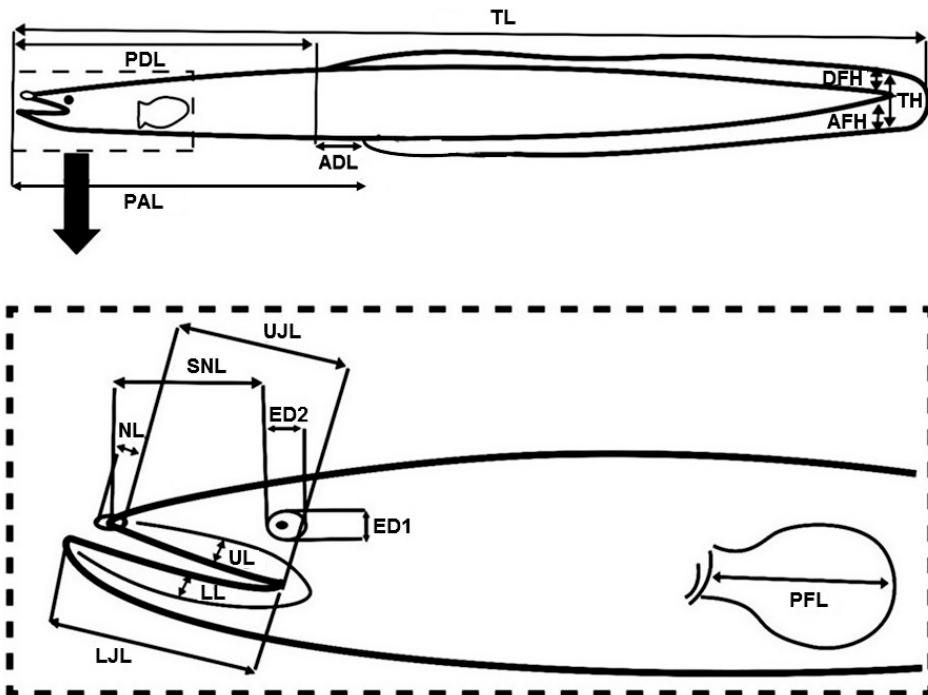


Fig. 3 Diagram showing morphological measurements of *Anguilla bicolor bicolor* from Segara Anakan, Indonesia.

Ano-dorsal length (ADL), Anal fin height (AFH), dorsal fin height (DFH), eye diameter, horizontal (ED2), eye diameter vertical (ED1), lower jaw length (LJJ), lower lip depth (LL), nostril length (NL), pectoral fin length (PFL), pre-anal fin length (PAL), pre-dorsal fin length (PDL), snout length (SNL), tail height (TH), upper jaw length (UJL), upper lip depth (UL) of *A. bicolor bicolor* from Segara Anakan in Cilacap, Central Java, Indonesia.

ured using analytical scales. Specimens with a body weight of < 510 g were measured to the nearest 0.01 g, while specimens with a body weight of > 510 g was measured to the nearest 1 g.

Fifteen morphometric measurements were incorporated into the present study and these were; ano-dorsal length (ADL), anal fin height (AFH), dorsal fin height (DFH), eye diameter vertical (ED1), eye diameter horizontal (ED2), lower jaw length (LJL), lower lip depth (LL), nostril length (NL), pre-anal fin length (PAL), pre-dorsal fin length (PDL), pectoral fin length (PFL), snout length (SNL), tail height (TH), total length (TL), upper jaw length (UJL) and upper lip depth (UL).

ADL was measured the distance between the origins of the dorsal and anus. TH, DFH and AFH were measured at 98% of TL and these were used to calculate: tail height to total length ratio (TI), $TI = 100 \frac{TH}{TL}^{-1}$, dorsal fin height to total length ratio (DFI), $DFI = 100 \frac{DFH}{TL}^{-1}$, anal fin height to total length ratio (AFI), $AFI = 100 \frac{AFH}{TL}^{-1}$. Measurements of PFL, SNL, NL, UL, LL, UJL, LJL were taken from the left side of specimens and were used to calculate pectoral fin length to total length ratio (PFI), $PFI = 100 \frac{PFL}{TL}^{-1}$, snout length to total length ratio (SNI), $SNI = 100 \frac{SNL}{TL}^{-1}$, nostril length to total length ratio (NI), $NI = 100 \frac{NL}{TL}^{-1}$, upper lip depth to total length ratio (UDI), $UDI = 100 \frac{UL}{TL}^{-1}$, lower lip depth to total length ratio (LDI), $LDI = 100 \frac{LL}{TL}^{-1}$, upper jaw length to total length ratio (UJI), $UJI = 100 \frac{UJL}{TL}^{-1}$, lower jaw length to total length ratio (LJI), $LJI = 100 \frac{LJL}{TL}^{-1}$. Measurements of ED1 and ED2 were used to calculate eye index (EI), $EI = 100 \pi \frac{ED1 + ED2}{TL}^{-1}$ [PANKHURST, 1982]. Fulton's condition factor (K) was calculated using the BW and TL and used to describe the condition of specimens, $K = 10^6 \frac{BW}{TL^3}$. Gonad

somatic index (GSI) was calculated as a percentage of body weight (GW), $GSI = 100 \frac{GW}{BW}^{-1}$.

Statistical analysis

Statistical analyses were performed on the data to compare variance of indices using Kruskal-Wallis test followed by Pairwise test using Benferroni correction to determine the level of significance between stages. Correlation between indices and developmental stages were analyzed using Kendall correlation. All statistical analyses were conducted using SPSS software version 24.0 (SPSS Inc., Chicago, IL, USA).

We further categorized morphological changes into three indices which were; development index, locomotion index and feeding behavior index. The development index included GSI and K, meant to indicate readiness to migrate to spawning locations. Locomotion index included TI, DFI, AFI, PFI and EI, meant to indicate changes to locomotory appendages as yellow eels which are benthic dwellers metamorphose to silver eels which are pelagic or mesopelagic swimmers and require optimal swimming capabilities to reach distant spawning locations. Feeding behavior index included NI, UJI, LJI, UDI, LDI and SNI, indicates changes to feeding appendages which gradually occur as silver eels stop feeding prior to migratory behavior.

3. Results

Observation of body color

From the 107 specimens in total, there were 68 males and 39 females. The present study was able to distinguish five developmental stages based on external morphological characters for both males and females (Fig. 4) and these were designated as: Y1, Y2, S1, S2 and S3. Morphological differences can be practically used in the field to distinguish between stages (Fig 5).

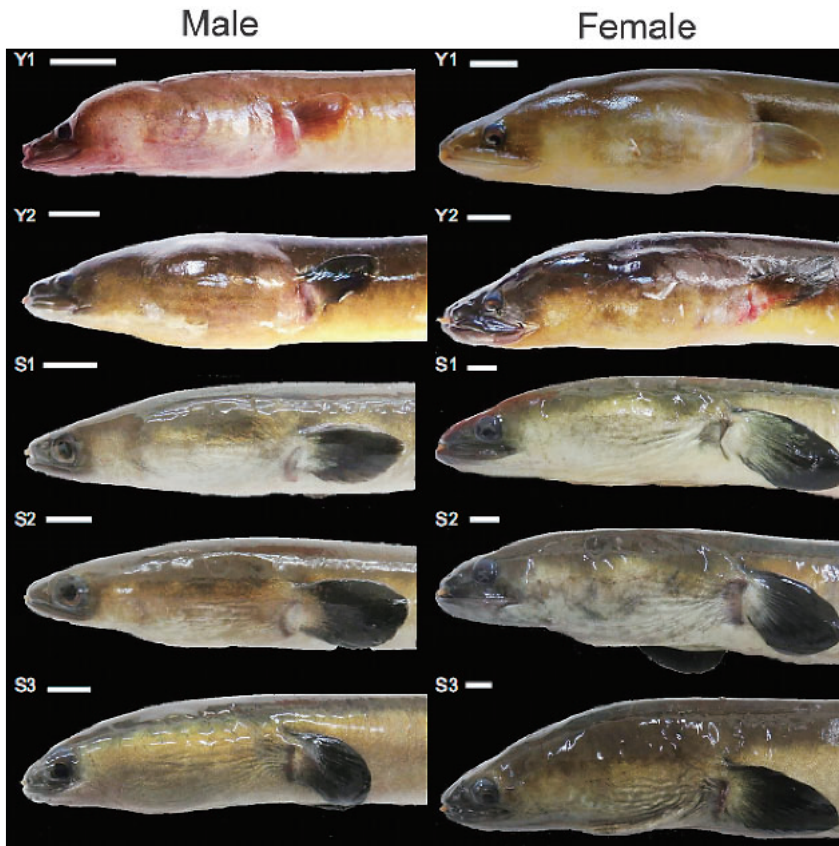


Fig. 4 Morphological characteristics of silvering stages based on body and pectoral fin coloration in males and females of *Anguilla bicolor bicolor* from Segara Anakan. For Y1, Y2, S1, S2 and S3, see text. Bar length 10 mm.

Y1 has a yellow colored belly, without metallic pigmentation. Pectoral fins without black coloration and the base of pectoral fins without metallic hue.

Y2 has similar coloration on belly and base of pectoral fins as Y1, but with black coloration on pectoral fins.

S1 has < 60% of belly covered with metallic pigmentation. Black color coverage on pectoral fins are $\leq 80\%$ and with < 50% metallic hue at the base of pectoral fins.

S2 has $\leq 80\%$ but $\geq 60\%$ of belly covered with metallic pigmentation and black color coverage of pectoral fins $\geq 50\%$ but $\leq 70\%$. Metallic hue at

the base of pectoral fins is similar to that of S1, < 50%.

S3 has > 80% metallic pigmentation on the belly with > 80% black color coverage of pectoral fins and > 70% metallic hue color at the base of pectoral fins.

There is an increasing trend in the percentage of metallic pigmentation (silver belly coloration), black color coverage of pectoral fins and metallic hue coverage at the base of pectoral fins with increase in silvering stages (Fig 6).

Y1 had a total of 30 specimens, with TL of males (n = 19) ranging from 265–384 mm and females (n = 11) from 390–513 mm, (Fig 6). Y2

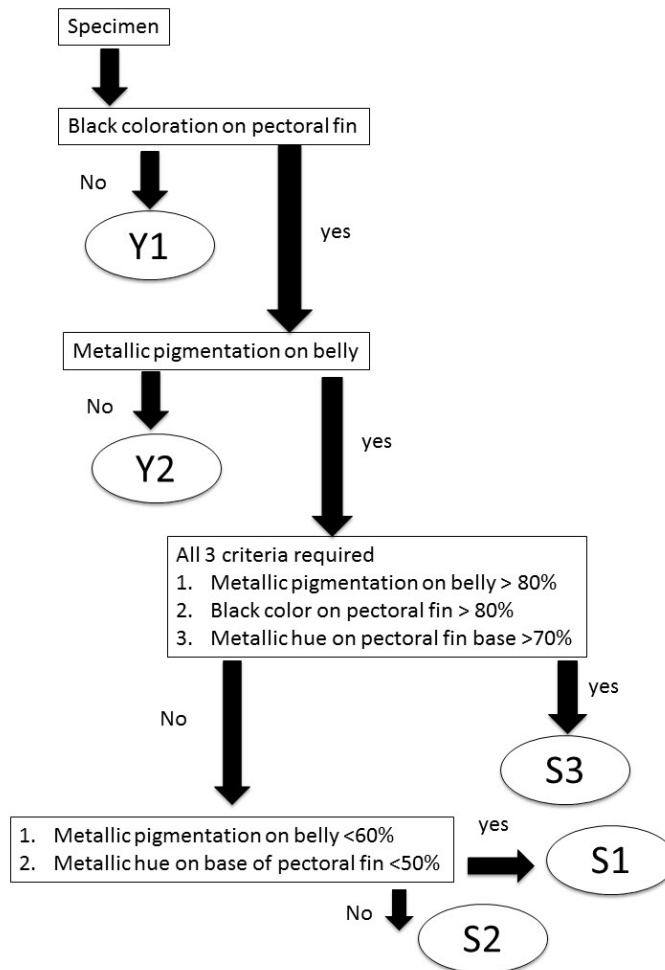


Fig. 5 Diagram showing morphological differences of color to distinguish between stages of females and males *Anguilla bicolor bicolor* from Segara Anakan, Indonesia

had 24 specimens with TL of males ($n = 14$) ranging from 327–429 mm, while females ($n = 10$) from 441–780 mm. S1 had 12 specimens with TL of males ($n = 6$) ranging from 350–442 mm and females ($n = 6$) from 674–799 mm. S2 had 20 specimens with TL of males ($n = 14$) ranging from 342–501 mm and females ($n = 6$) from 702–829 mm. Finally S3 had 21 specimens with TL of males ($n = 15$) ranging from 409–496 mm and females ($n = 6$) from 785–937 mm.

Morphological measurement

Based on Kruskal Wallis test, there were significant differences of the following indices between the various silvering stages in males and females ($P < 0.01$); K, GSI, TI, DFI, AFI, PFI, EI, and NI, in males only ($P < 0.01$); UJI and LJI and in females only ($P < 0.05$); LDI. While there were no significant differences of UDI and SNI. TL of males were notably smaller than females and ranged from 342 mm–501 mm with mean \pm

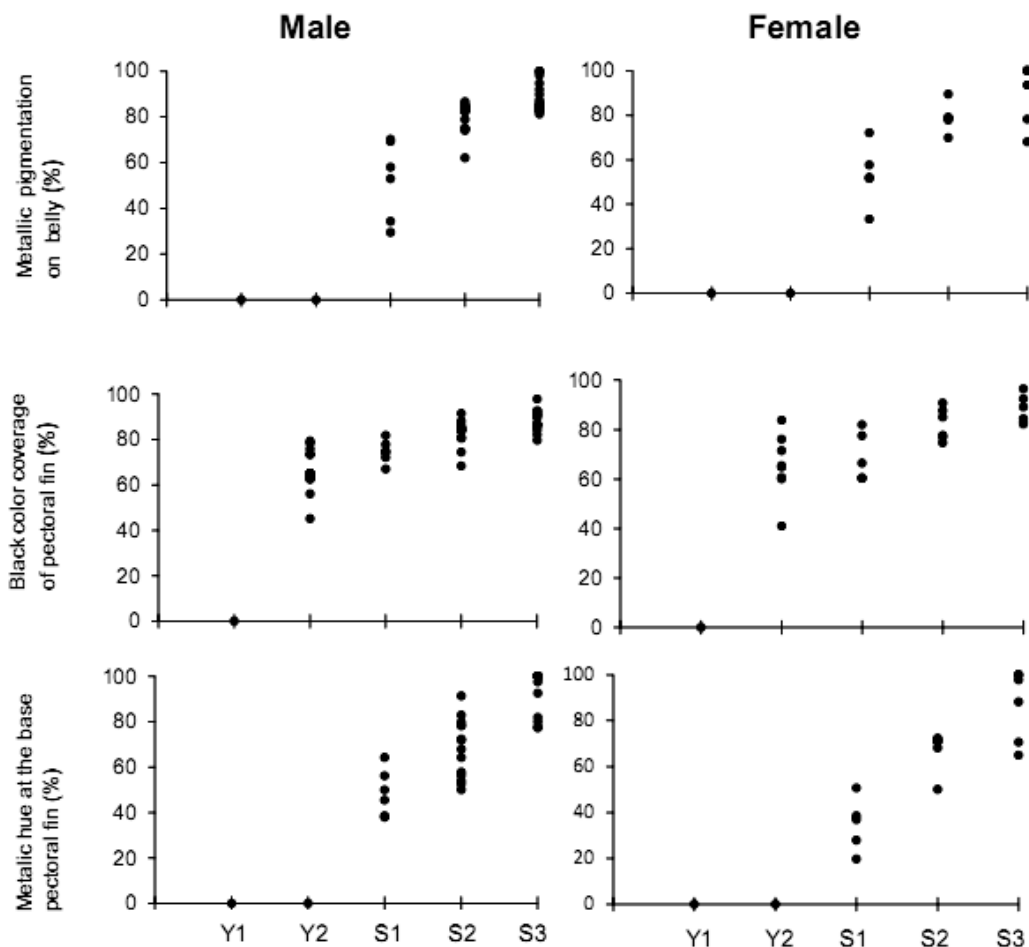


Fig. 6 Percentage of silver belly coloration, black color coverage of pectoral fin, and metallic hue at the base of pectoral fin in silvering stages of male and female *Anguilla bicolor bicolor* from Segara Anakan, Indonesia.

SD of 414.83 ± 40.38 mm, while that of females ranged from 674 mm–937 mm (786.11 ± 68.98 mm).

Development index

For both male and female *A. bicolor bicolor* there was a trend of a gradual increase in K and GSI with progression of silvering stages (Fig. 7). In male silver stages (S1–S3) displayed significantly higher K and GSI compared to Y1 stages. Y2 was observed to have significantly lower GSI

compared to S2 and S3. For both male and female there was no significantly differences K and GSI between three silver stages (S1–S3) ($P < 0.05$). Based on Kendall correlation, K and GSI showed strong positive correlations between silvering stages in both males and females ($P < 0.01$).

Locomotion index

There was a general increase of locomotion indices (TI, DFI, AFI, PFI, and EI) with incre-

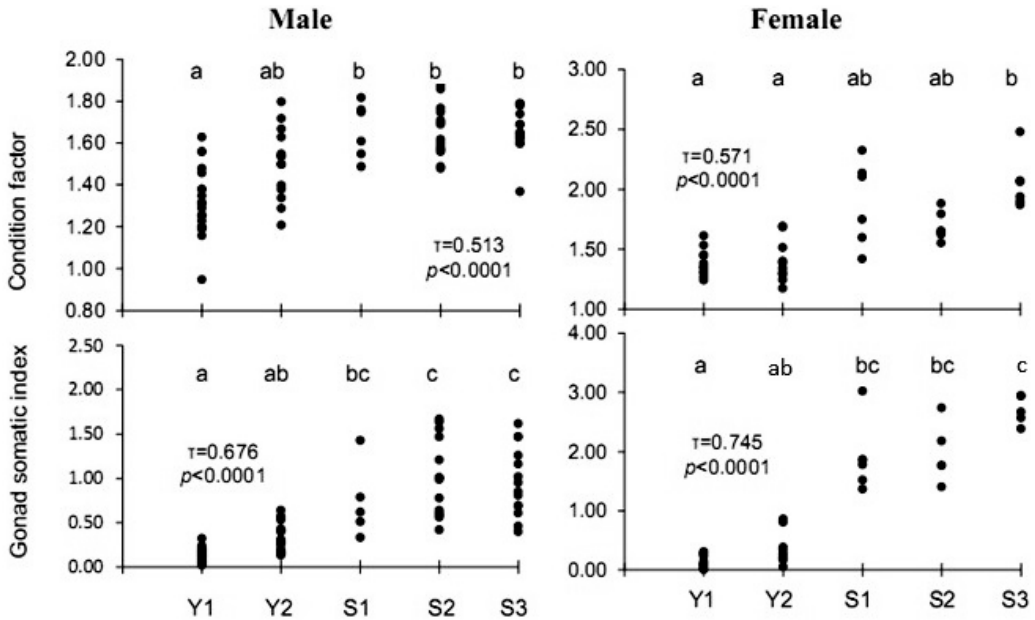


Fig. 7 The development indices in silvering stages of male and female *Anguilla bicolor bicolor* from Segara Anakan, Indonesia.

ment of stages in both males and females (Fig. 8). In males all five locomotion indices (TI, DFI, AFI, PFI and EI) within silver stages (S1–S3) were significantly higher than those of Y1. All indices of Y2 were significantly lower than those of S2 and S3 ($P < 0.05$).

In females all five locomotion indices of Y1 had significantly lower than those of S1 and S2. S3 was observed to have significantly higher AFI, PFI and EI compared to Y1. Y2 was significantly lower TI, DFI, AFI than those of S1 and S2. S3 was observed to have significantly higher TI, AFI, EI compared to Y2 ($P < 0.05$). Based on Kendall correlation, both males and females showed positive correlation between locomotion indices and developmental stages ($P < 0.01$).

Feeding behavior Index

In males the UJI and LJI of S3 were significantly higher than those of Y1. NI of Y1 was significantly higher than that of Y2 and S2. Y2 dis-

played significantly higher NI compared to S2 ($P < 0.05$). Based on Kendall correlation, UJI and LJI showed positive correlation with developmental stages, while negative correlation between NI and developmental stages ($P < 0.01$) (Fig. 9).

In females S3 was significantly lower NI and LDI than those of Y1. NI of Y2 was significantly higher than that of S3. Based on Kendall correlation, NI and LDI showed negative correlation with developmental stages ($P < 0.01$) (Fig. 9).

Seasonal occurrence

Silvering females were caught during most months of the year (Table 1), while silvering males were only caught during May 2017 and May–June 2018. Silvering females were also observed in both the wet months of the year (December to March) and dry months (May to June) in Segara Anakan with corresponding peak season for females the same as males which was in

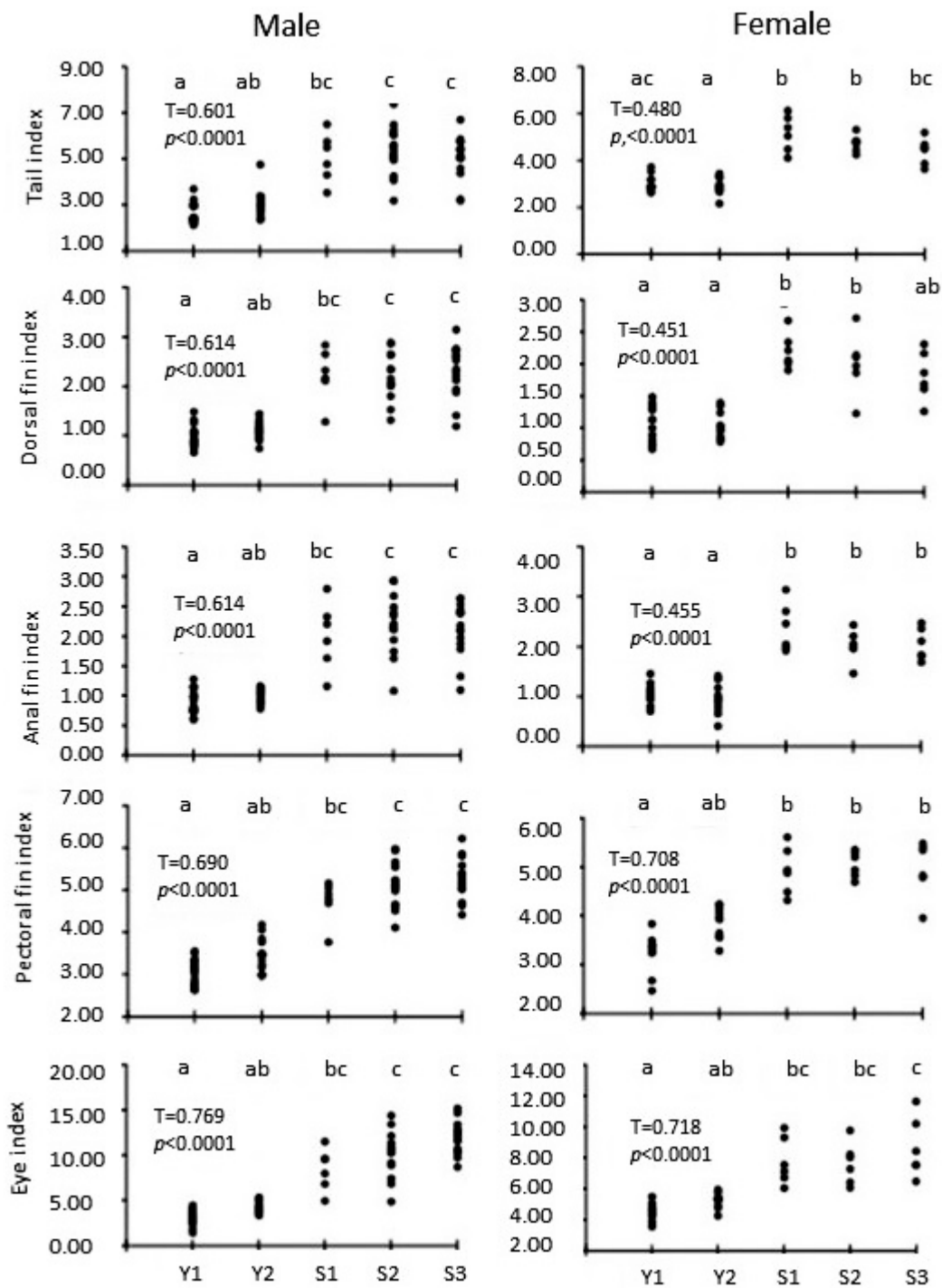


Fig. 8 The locomotion indices in silvering stages of male and female *Anguilla bicolor bicolor* from Segara Anakan, Indonesia.

Table 1. Catch date, total length and body weight of silver phase *Anguilla bicolor bicolor* used in present study

Date	Sex	Sample size (n)	Total length (mm)		Body weight (g)		Season
			range	mean \pm SD	range	mean \pm SD	
Dec 31th, 2015	F	1	818		905		R
Jan 29th, 2016	F	1	937		1565		R
Feb 1st, 2016	F	1	908		1400		R
May 18th, 2016	F	1	810		1100		D
Aug 27th, 2016	F	1	785		1200		D
Sep 19th, 2016	F	1	745		870		D
May 4th, 2017	F	3	702-829	754.67 \pm 66.21	533-935	801.33 \pm 215.27	D
May 5th, 2017	M	29	342-501	430.10 \pm 39.50	83-199	134.50 \pm 35.17	D
May 10th, 2017	F	9	674-866	764.78 \pm 54.94	537-1339	815.70 \pm 226.79	D
May 23th, 2018	M	5	350-456	430.10 \pm 134.50	78-160	134.50 \pm 35.17	D
June 2nd, 2018	M	1	450		125		D

R: Rainy season, D: Dry season

May 2017 and 2018, during the dry months.

4. Discussion

Body and pectoral fin coloration in silvering stages

The present study is the first to identify the difference in size of silvering female and male *A. bicolor bicolor* and categorize the silvering stages of both sexes collected from Segara Anakan in Indonesia based on body and pectoral fin coloration into 5 stages: Y1, Y2, S1, S2 and S3. When comparing the 5 silvering stages of *A. bicolor bicolor* of the present study to similar studies, OKAMURA *et al.* (2007) and HAGIHARA *et al.* (2012) demarcated silvering stages of *A. japonica* in Mikawa Bay, Japan and *A. celebesensis*, in Poso Lake, Sulawesi Indonesia respectively into 4 stages: Y1, Y2, S1 and S2. Furthermore HAGIHARA *et al.* (2012) also described the silvering stages of *A. marmorata* from the same area which were grouped into 3 stages: Y1, Y2, and S1. The silvering stages of female *A. bicolor bicolor* from Segara Anakan, Indonesia reported

by ARAI *et al.* (2016) and female *A. bicolor bicolor* and *A. bengalensis bengalensis* from Penang, Malaysia (ARAI and ABDUL KADIR, 2017) were grouped into 5 stages but these were based on the development of GSI and gonad histology. Additionally, male *A. bicolor bicolor* from Penang, Malaysia was grouped into 3 stages and male *A. bengalensis bengalensis* into 2 stages by ARAI and ABDUL KADIR (2017). Discrimination of silvering eels employing gonadal histology is invasive, therefore a more practical method utilizing external morphological characters such as body and pectoral fin coloration presented in the present study will enable easy identification for monitoring studies within the South-east Asian region.

The synchronous development of silver coloration on the body and pectoral fins together with the maturation of gonads which were observed for tropical eel *A. bicolor bicolor* of the present study have also been observed in several species of temperate eels: *A. japonica* (HAN *et al.*, 2003; OKAMURA *et al.*, 2007), *A. anguilla* (DURIF *et al.*,

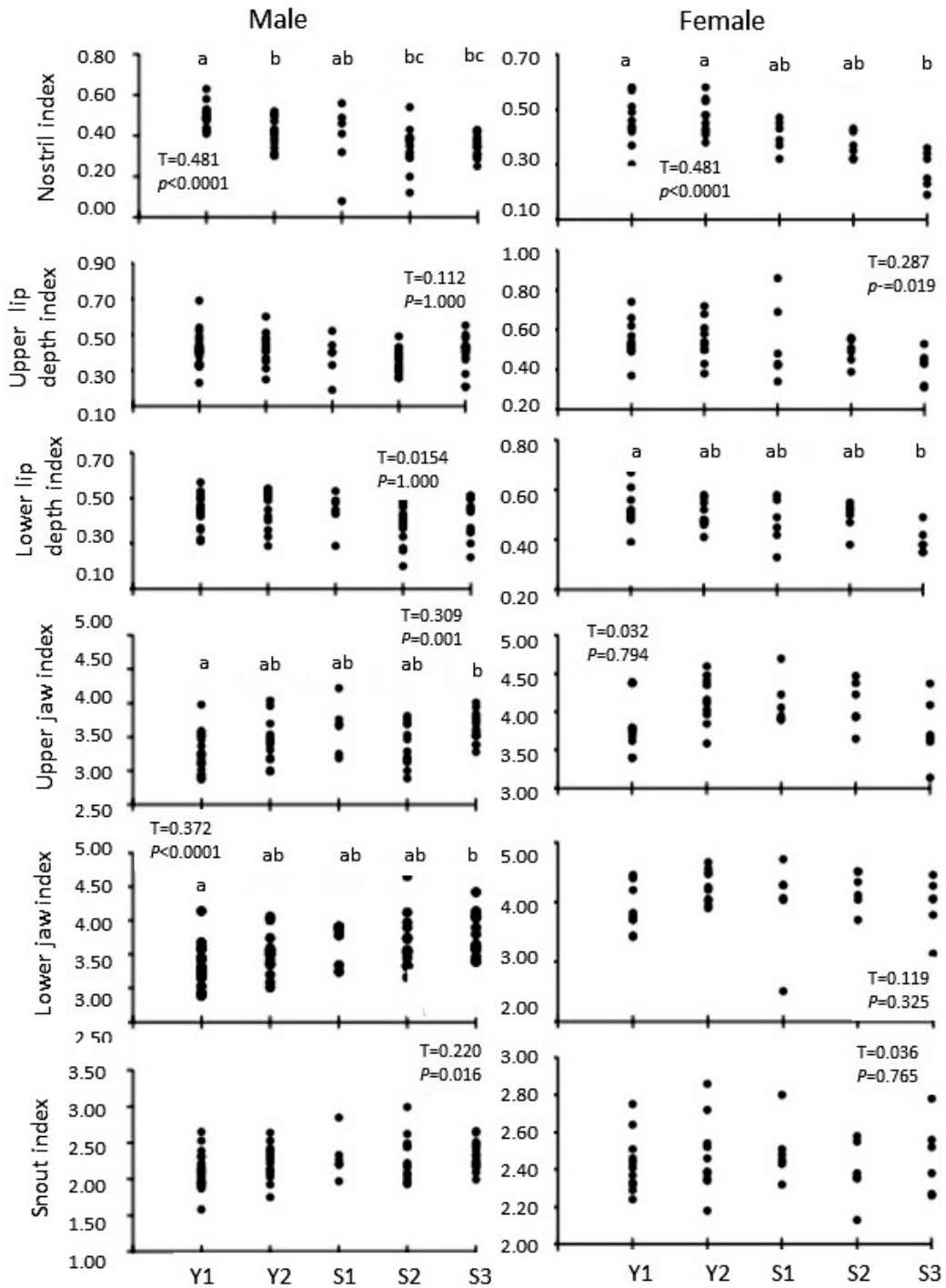


Fig. 9 The feeding behavior indices in silvering stages of male and female *Anguilla bicolor bicolor* from Segara Anakan, Indonesia.

2005), *A. dieffenbachii*, *A. australis* (TODD, 1981) and other tropical eels: *A. bicolor bicolor*, (ROBINET and FEUNTEUN, 2002), *A. celebesensis* and *A. marmorata* (HAGIHARA *et al.*, 2012). Both temperate and tropical anguillid eels displayed similar morphological development during the silvering process with dorsal regions developing black coloration while ventral regions a metallic silver coloration. The pectoral fins also developed darker coloration until the distal portion of the base of the pectoral fin which displayed golden or silver coloration. (TODD, 1981; ROBINET and FEUNTEUN, 2002; DURIF *et al.*, 2005; OKAMURA *et al.*, 2007; HAGIHARA *et al.*, 2012). HAN *et al.* (2003) suggested that these changes in skin coloration were highly correlated with gonadal development in Japanese eels and therefore the external morphological changes observed in the present study for *A. bicolor bicolor* supports that suggestion.

Morphological and physiological changes

Firstly the development indices of the present study, K and GSI were observed to increase with the increase of silvering stages (Fig. 7). DURIF *et al.* (2005) reported similar results for *A. anguilla* and suggested that with increasing sexual maturity, anguillid eels tend to increase in size and K. In most species of anguillid eels it has been reported that female eels tend to maximize their size, i. e. K, in order to maximize fecundity (WENNER and MUSICK, 1974; VOLLESTAD and JONSSON, 1986; HELFMAN *et al.*, 1987). For large *A. anguilla*, DURIF *et al.* (2006) observed that gonad weight (GSI) increased exponentially with size at maturation and that larger silver eels developed proportionally more gonads as compared to smaller silver eels, suggesting that an increase in K would facilitate greater reproductive success. DURIF *et al.* (2006) further reported that K or fat content of female eels directly impacts the ca-

capacity for egg production and also provides energy reserves for spawning migrations. Although there was no significant increase of GSI expressed in the present study, there is a noticeable increasing trend of GSI with sexual maturity. This is similar to those of several studies (TODD, 1981; HAN *et al.*, 2003; DURIF *et al.*, 2006). In *A. anguilla*, DURIF *et al.*, (2006) reported that maturation was characterized by the weight of gonads which in turn reflected fecundity. TODD (1981) further reported that higher GSI values in *A. australis* and *A. dieffenbachii* displayed greater oocyte diameter while ARAI and KADIR (2017) stated that tropical eels, *A. bengalensis* and *A. bicolor bicolor* both displayed greater development of the gonad structure with increase in GSI. Therefore it is clear that increasing development indices with increasing sexual maturity observed for *A. bicolor bicolor* in the present study correlates to an adaptive feature which would enable greater reproductive success and migration success and is typical for most anguillid eels.

Secondly, locomotion indices of the present study (Fig. 8) displayed a general increasing trend of all indices from early yellow stages to late silver stages. The increase in PFI is an important adaptation for anguillid eels during their spawning migrations as pectoral fins act as stabilizers and aids in predator avoidance (HAGIHARA *et al.*, 2012). The present study is also the first to provide information on DFI, AFI and TI for anguillid eels which displayed increasing trends with increase in silvering stages. Increase in all aspects of the caudal fin region i.e. DFI, AFI and TI will improve swimming ability during spawning migration (MULLER *et al.*, 2001). Furthermore the EI of *A. bicolor bicolor* in our study also displayed an increasing trend of 3.82-folds in males and 1.78-folds in females with increasing sexual maturity from yellow to silver stages (Fig. 7). The increase in size of the eyes (EI) in the

present study may also function in aiding of predator detection during oceanic migrations to spawning locations. This has also been observed for several other species of anguillid eels such as *A. australis*, *A. dieffenbachii* (TODD, 1981) and *A. anguilla* (NOWOSAD *et al.*, 2014). The present study was also the first to provide silvering indices for males of *A. bicolor bicolor* from Indonesia. The EI of late silver males in this study (11.92 ± 1.75) was also found to be considerable higher than other anguillid eels, *A. bengalensis bengalensis* and *A. bicolor bicolor* from Malaysia (6.09 ± 1.08 and 7.65 ± 2.49 , respectively) (ARAI and ABDUL KADIR, 2017), *A. japonica* (5.7 ± 0.6) (YOKOUCHI *et al.*, 2009) and *A. anguilla* (9.9 ± 1.6) (DURIF *et al.*, 2005).

The feeding behavior index, i.e. UDI, and SNI of *A. bicolor bicolor* of both sexes in this study did not display degeneration with progression of silvering stages from Y1 to S3. UJI and LJI in males showed the increasing trend with progression of silvering stages, while LDI in females showed the decreasing trend with progression of silvering stages. NI in both males and females showed the decreasing trend with progression of silvering stages (Fig. 9). Furthermore all samples for this study including late stage silver eels were lured and collected using baited traps and hooks. These results suggest that silver eels of *A. bicolor bicolor* from Segara Anakan were feeding individuals even at late stage (S3) silver eels. This is in contrast to temperate eels such as *A. anguilla*, *A. rostrata* and *A. japonica*. DURIF *et al.* (2005) reported that *A. anguilla* ceased feeding at the onset of silver eel maturation, which resulted in degeneration of the gut. PANKHURST and SORESENSEN (1984), LIONETTO *et al.* (1996) and OKAMURA *et al.* (2007) also observed similar degeneration of the elementary tract in silver eels of *A. anguilla*, *A. rostrata* and *A. japonica* respectively. This degeneration may also be a result of

cessation in feeding. We suggest that *A. bicolor bicolor* may be feeding individuals right up until they begin oceanic migrations. Furthermore it is possible that *A. bicolor bicolor* cease feeding as soon as oceanic migration commences as evident through the decrease in NI. Nostrils of anguillid eels are connected to the olfactory organ which plays an important role in the location of feed (ATTA, 2013). Therefore a decrease in NI with sexual maturity suggests that although late stage silver eels feed within continental waters they may cease feeding at the onset of oceanic migration. With very few studies on silvering stages of tropical eels and even fewer on comparison of feeding behavior indices of tropical silver eels it is important that similar studies are conducted on other tropical anguillid species to verify if this hypothesis is common for other tropical species.

Although silver eel collections during the present study were conducted intermittently by local fishermen, a seasonal trend could be observed for both males and females. Female silver eels were observed relatively throughout the year in low numbers with peak collection periods during the dry season in May 2017 and 2018. This is typical for tropical anguillid eels which have been suggested to spawn throughout the year (KUROKI *et al.*, 2009). Males however were only collected during the dry months of the year, in May 2017 and May-June 2018, of 35 samples which also corresponds to peak collection seasons for females (Table 1). As there may have been shortcomings with the frequency and effort of eel collection by fishermen, it is entirely possible that males were also present during the year but were simply not collected. Additionally it may be fairly assumed that peak silver eel migration periods of *A. bicolor bicolor* in the Segara Anakan are during the dry seasons around May. Temperate anguillid eels *A. japonica* (MATSUI, 1957),

A. rostrata (JESSOP, 1987), *A. anguilla* (VOLLESTAD *et al.*, 1986), *A. australis* and *A. dieffenbachii* (TODD, 1981; SLOANE, 1984; JELLYMAN, 1987) all make their spawning migrations either during fall or winter seasons. VOLLESTAD *et al.* (1986) further reported that high water discharge and low temperature were the main factors influencing the onset of *A. anguilla* silver eel runs. Therefore peak silver eel runs for *A. bicolor bicolor* from Segara Anakan seem to be triggered by low temperatures rather than rainfall, as dry seasons are also relatively cold seasons in the Java region and this is when majority of silver eels were captured in the present study. Average temperatures and rainfall per month during May-August 2017 was 30 °C and 122 mm respectively, compared to 32 °C and 375 mm respectively for September 2017–April 2018 (Indonesian Central Bureau of Statistics, 2019a,b). Contraction of habitat and reduction of resource availability brought on by dry seasons may trigger eels in Segara Anakan to commence spawning migrations.

The present study was able to provide information on the morphological differences of silvering stages in *A. bicolor bicolor* of both sexes from the Segara Anakan Estuary. Two yellow eel and three silver eel stages were differentiated using clear and easily distinguishable external morphological characters. An identification key using external morphological features presented in this study will enable fisheries agencies to quickly and conveniently distinguish the various silver eel stages. This will abate in the monitoring of silver eel migration patterns in the region and assist in conservation programs aimed at effectively utilizing this species. The present study was only able to collect samples from fishermen when they were available and a more systematic approach is required to obtain a more robust understanding of the abundance

and seasonality of *A. bicolor bicolor* silver eel migrations in the Segara Anakan Estuary. Currently this species is listed as 'near threatened' by the IUCN Red List of Threatened Species (JACOBY *et al.*, 2014) and further life history studies are required for the promulgation of effective conservation programs in the future.

Acknowledgements

The authors would like thank all the SIDAT team namely Adhi Prasetyo, Ariel Hanaya, Christin Ratucoreh, Juniari Saraswati, Oa Etty Kerans and Rika Trianasari in Animal Structure and Development Laboratory, Biology Faculty of Universitas Gadjah Mada who helped us collect the samples. Bpptnbh Biology Faculty, Universitas Gadjah Mada which supported this research through funding.

References

- AOYAMA, J., S. WOUTHUYZEN, , M. J. MILLER, Y. MINEGISHI, M. KUROKI, S. R. SUHARTI, T. KAWAKAMI, K. O. SUMARDIHARGA, and K. TSUKAMOTO (2007): Distribution of leptocephali of the freshwater eels, genus *Anguilla*, in the waters off west Sumatra in the Indian Ocean. *Environmental Biology of Fishes*, **80**, 445–452.
- ARAI, T., S. R. ABDUL KADIR, and N. CHINO (2016): Year round spawning by a tropical catadromous eel *Anguilla bicolor bicolor*. *Marine Biology*, **163**, 1–7.
- ARAI, T., and S. R. ABDUL KADIR (2017): Opportunistic spawning of tropical anguillid eels *Anguilla bicolor bicolor* and *A. bengalensis bengalensis*. *Scientific Reports*, **7**, 1–17.
- ATTA, K. I. (2013): Morphological, anatomical and histological studies on the olfactory organs and eyes of teleost fish: *Anguilla anguilla* in relation to its feeding habits. *The Journal of Basic & Applied Zoology*, **66**, 101–108.
- BERTIN, L. (1956): 'Eel: A Biological Study'. pp. 6–54. (Cleaver Human Press: Paris, Franch)
- BOWMAKER, J. K., M. SEMO, D. M. HUNT., and G. JEFFERY

- (2008): Eels visual pigments revisited: The fate of retinal cones during metamorphosis. *Visual Neurosciences*, **25**, 249–255.
- DURIF, C., S. DUFOUR, and P. ELIE (2005): The silvering process of *Anguilla anguilla*: a new classification from the yellow resident to the silver migrating stage. *Journal of Fish Biology*, **66**, 1025–1043.
- DURIF, C. M. F., S. DUFOUR, and P. ELIE (2006): Impact of silvering stage, age, body size, and condition on reproductive potential of the European eel. *Marine Ecology Progress Series*, **327**, 171–181.
- EGE, V. (1939). A revision of the genus *Anguilla* Shaw, a systematic, phylogenetic and geographical study. *Dana Rep.* **16**, 1–256.
- EGGINTON, S. (1986): Metamorphosis of the American eel, *Anguilla rostrata* Le Seur: I. changes in metabolism of skeletal muscle. *The Journal of Experimental Zoology*, **237**, 173–184.
- FUKUDA, N., M. J., MILLER, J., AOYAMA, A. SHINODA, and K. TSUKAMOTO (2013): Evaluation of the pigmentation stages and body proportions from the glass eel to yellow eel in *Anguilla japonica*. *Fisheries Science*, **79**, 425–438.
- HAGIHARA, S., J. AOYAMA, D. LIMBONG, and K. TSUKAMOTO (2012): Morphological and physiological changes of female tropical eels, *Anguilla celebesensis* and *Anguilla marmorata*, in relation to downstream migration. *Journal of Fish Biology*, **81**, 408–426.
- HAN, Y., I. LIAO, Y. HUANG, J. HE, C. CHANG, and W. TZENG (2003): Synchronous changes of morphology and gonadal development of silvering Japanese eel *Anguilla japonica*. *Aquaculture*, **219**, 783–796.
- HELFMAN, G. S., D. E. FACEY, S. HALES, and E. L. BOZEMAN (1987): Reproductive ecology of the American eel. In: DADSWELL, M. J., R. J. KLAUDDA, C. M. MOFFIT, R. I. SAUNDERS, R. A. RULIFSON, J. E. COOPER (eds) *Common strategies of anadromous and catadromous fishes*. pp. 286–29. (American Fisheries Society: Bethesda, Massachusetts).
- Indonesian Central Bureau of Statistics (Biro Pusat Statistik). (2019a). Suhu udara di Stasiun Pengamatan BMKG Kabupaten Cilacap (derajat C), 2010–2017. <https://cilacapkab.bps.go.id/dynamictable/2016/09/08/155/suhu-udara-di-stasiun-pengamatan-bmkg-kabupaten-cilacap-derajat-c-2010-2017.html>
- Indonesian Central Bureau of Statistics (Biro Pusat Statistik). (2019b). Banyaknya curah hujan, curah hujan terbesar, dan banyaknya hari hujan menurut bulan di Kabupaten Cilacap, 2010–2017. <https://cilacapkab.bps.go.id/dynamictable/2016/09/08/154/banyaknya-curah-hujan-curah-hujan-terbesar-dan-banyaknya-hari-hujan-menurut-bulan-di-kabupaten-cilacap-2010-2017.html>
- JACOBY, D. M. P., I. J. HARRISON, and M. J. GOLLOCK (2014). *Anguilla bicolor*. The IUCN Red List of Threatened Species 2014: e. T166894A6701570. <http://dx.org/10.2305/IUCN.UK.2014-1.RLTS.T166894A67015719.en>.
- JELLYMAN, D. J. (1987). Review of the marine life history of Australasian temperate species of *Anguilla*. *American Fisheries Society Symposium*, **1**, 276–285.
- JESSOP, B. M. (1987). Migrating American eels in Nova Scotia. *Transactions of the American Fisheries Society*, **116**, 161–170.
- KUROKI, M., J. AOYAMA, M. J. MILLER, T. YOSHINAGA, A. SHINODA, S. HAGIHARA, K. TSUKAMOTO (2009). Sympatric spawning of *Anguilla marmorata* and *Anguilla japonica* in the western North Pacific Ocean. *Journal of Fish Biology*, **74**, 1853–1865.
- LARSSON, P., S. HAMRIN, and L. OKLA (1990): Fat content as a factor inducing migratory behavior in the eel (*Anguilla anguilla* L.) to the Sargasso Sea. *Naturwissenschaften*, **77**, 488–490.
- LIONETTO, M. G., M. MAFFIA, F. VIGNES, C. STORELLI, and T. SCETTINO (1996). Differences in intestinal electrophysiological parameters and nutrient transport rates between eels (*Anguilla anguilla*) at yellow and silver stages. *Journal of Experimental Zoology*, **275**, 399–405
- MATSUI, I. (1957). On the record of a leptocephalus and catadromous eels of *Anguilla japonica* in the waters around Japan with a presumption of their spawning places. *Journal of the Shimonoseki College of Fisheries*, **7**, 151–167
- MINEGISHI, Y., J. AOYAMA, J. G. INOUE, M. MIYA, M.

- NISHIDA, and K. TSUKAMOTO (2005): Molecular phylogeny and evolution of the freshwater eels genus *Anguilla* based on the whole mitochondrial genome sequences. *Molecular Phylogenetics and Evolution*, **34**, 134-146.
- MULLER, U. K., J. SMIT, E.J. STAMHUIS, and J. J. VIDELER (2001). How the body contribute to the wake in undulatory fish swimming: Flow fields of a swimming eel (*Anguilla anguilla*). *Journal of Experimental Biology*, **204**, 2751-2762.
- NOWOSAD, J., D. KUCHARCZYK, T. K. CZARKOWSKI, and K. KWASEK (2014): Changes in body weight and eye size in female and European eel kept in fresh and salt water. *Italian Journal of Animal Science*, **13**, 382-386.
- OKAMURA, A., Y. YAMADA, K. YOKOUCHI, K. N. HORIE, N. MIKAWA, T. UTOH, S. TANAKA, and K. TSUKAMOTO (2007): A silvering index for the Japanese eel *Anguilla japonica*. *Environmental Biology of Fishes*, **80**, 77-89.
- PANKHURST, N. W. (1982): Relation of visual changes to the onset of sexual maturation in the European eel *Anguilla anguilla* L. *Journal of Fish Biology*, **21**, 127-140.
- PANKHURST, N. W. and P. W. SORENSON (1984). Degeneration of the alimentary tract in sexually maturing European *Anguilla anguilla* (L.) and American eels *Anguilla rostrata* (LeSueur). *Canadian Journal of Zoology*, **62**, 1143-1148
- ROBINET, T., and E. FEUNTEUN (2002): First observation of shortfinned *Anguilla bicolor bicolor* and longfinned *Anguilla marmorata* silver eels in the Reunion Island. *Bulletin Francais de la Peche et de la Pisciculture*, **364**, 87-95.
- SLOANE, R. D. (1984). Preliminary observations of migrating adult freshwater eels (*Anguilla australis australis* Richardson) in Tasmania. *Australian Journal of Marine and Freshwater Research*, **35**, 471-476.
- SUGEHA, H. Y., S. R. SUHARTI, S. WOUTHUYZEN, and K. SUMADHIHARGA (2008): Biodiversity, distribution and abundance of the tropical anguillid eels in the Indonesian waters. *Marine Research Indonesia*, **33**, 129-137.
- SVEDANG, H., and H. WICKSTROM (1997): Low fat contents in female silver eels: indications of insufficient energetic stores for migration and gonadal development. *Journal of Fish Biology*, **50**, 475-486.
- TAWA, A., M. KOBAYAKAWA, T. YOSHIMURA, and N. MOCHIOKA (2012): Identification of leptocephalus larvae of the tiger moray *Scuticaria tigrina* (Anguilliformes; Muraenidae) based on morphometric and genetic evidence. *Ichthyological Research*, **59**, 378-383.
- TESCH, F. W. (1980): Occurrence of eel *Anguilla anguilla* larvae west of the European Continental Shelf, 1971-1977. *Environmental Biology of Fishes*, **5**, 185-190.
- TESCH, F. W. (2003): 'The Eel.' Third Edition (Eds J. E. Thorpe) pp. 13-17. (Blackwell Science: British).
- TODD, P. R. (1981): Morphometric changes, gonad histology, and fecundity estimates in migrating New Zealand freshwater eels (*Anguilla* spp.). *New Zealand Journal of Marine and Freshwater Research*, **15**, 155-170.
- VOLLESTAD, L. A. and B. JONSSON (1986): Life-history characteristics of the European eel *Anguilla anguilla* in the Imsa River, Norway. *Transaction of the American Fisheries Society*, **115**, 864-871.
- VOLLESTAD, L. A., B. JONSSON, N. A. HVIDSTEN, T. F., NAESJE, Ø. HERALSTAD, J. RUUD-HANSEN (1986). Environmental Factors Regulating the Seaward Migration of European Silver Eels (*Anguilla anguilla*). *Canadian Journal of Fisheries and Aquatic Sciences*, **43**, 1909-1916.
- WENNER, C. A., and J. A., MUSICK (1974): Fecundity and gonadal observations of the American eel, *Anguilla rostrata*, migrating from Chesapeake Bay, Virginia. *Journal of the Fisheries Research Board of Canada*, **31**, 1387-1391.
- YAMADA, Y., H. ZHANG, A. OKAMURA, S. TANAKA, N. HORIE, N. MIKAWA, T. UTOH, and P. OKA (2001). Morphological and histological changes in the swim bladder during maturation of the Japanese eel. *Journal of Fish Biology*, **58**, 804-814.
- YOKOUCHI, K., R. SUDO, K. KAIFU, J. AOYAMA, and K. TSUKAMOTO (2009): Biological characteristics of silver-phase Japanese eels, *Anguilla japonica*,

collected from Hamana Lake, Japan. Coastal Marine Science, **33**, 54-63.

Received: May 24, 2019

Accepted: October 10, 2019

アリアケシラウオはどこで産卵するのか?

東島昌太郎*・木下 泉・広田祐一

Where do the salangid, *Salanx ariakensis* endemic to Ariake Bay in Japan spawn?

Shotaro TOJIMA*, Izumi KINOSHITA and Yuichi HIROTA

Abstract: Little is known about the early life history of critically endangered salangid, *Salanx ariakensis*, being one of the largest species in salangids, endemic to Ariake Bay in Japan. When surveying fish larvae and juveniles by a larva net and a beam trawl in Ariake Bay during spring tide period of December 2017, the larva net could yield a total of 10 yolk-sac, 10 preflexion, seven flexion and four postflexion larvae. No larvae occurred in any stations of rivers, and particularly the yolk-sac and preflexion larvae had been aggregated in waters around the mouth of each river. After starting the notochord flexion, they had tended to disperse westward along coasts with growth by the residual current, and to be nursed in shallow coasts with relatively polyhaline and less turbid waters for Ariake Bay. These phenomena could be found also in autumn of 2014, 2015 and 2016. Considering these information, it is likely that *S. ariakensis* spawn in the vicinity littorals of estuaries rather than the upper reach of rivers, as well as common salangid, *Salangichthys microdon*.

Keywords: *Salanx ariakensis*, larva, spawning ground, Ariake Bay

1. 緒言

有明海産のシラウオ科 Salangidae 魚類 3 種 (アリアケヒメシラウオ *Neosalanx reganius* Wakiya

and Takahashi, 1937, アリアケシラウオ *Salanx ariakensis* Kishinouye, 1902 およびシラウオ *Salangichthys microdon* (Bleeker, 1860)) (WAKIYA and TAKAHASHI, 1937; 日比野ほか, 2002b; 細谷, 2013) の内, 前二者は日本において有明海にのみ分布し (WAKIYA and TAKAHASHI, 1937), 環境省レッドリストにおいて絶滅危惧 IA 類に選定されている (小早川, 2015)。特に, アリアケシラウオは本邦に分布するシラウオ科中, 最大となり, 沿岸域から河川感潮域まで分布し, その資源量は著しく減少しているが (小早川, 2015), 本種の生活史, 特に再生産に関する情報は断片的または不十分なものしかない。その中で, 本種の産卵場につ

高知大学海洋生物研究教育施設

〒781-1164 高知県土佐市宇佐町井尻 194

Usa Institute of Marine Biology, Kochi University,
Usa, Tosa, Kochi 781-1164, Japan

* 連絡著者: 東島昌太郎

〒781-1164 高知県土佐市宇佐町井尻 194 高知大学海洋生物研究教育施設

Tel: 088-856-0633

Fax: 088-856-0425

E-mail: b17d6c04@s.kochi-u.ac.jp

Table 1. Collection records of *Salanx ariakensis* larvae by a larva net in Ariake Bay in November 2014 and 2015, and December 2016 and 2017. A, yolk-sac larva; B, preflexion larva; C, flexion larva; D, postflexion larva.

Date	Year	Stn. in Fig. 1	Collected number	Parameters at surface		Developmental stage	BL (mm)
				Salinity	Turbidity		
23, 24 Nov.	2014	37, 38, 54	3	27.0-29.7	4.1-13.2	B, C	6.3-12.2
25, 26 Nov.	2015	37, 52-54	7	23.2-28.3	12.2-49.6	B, C	9.8-14.7
13, 15, 17 Dec.	2016	6-8, 37, 66	14	24.9-29.6	6.4-51.0	A-D	6.2-20.6
3-5 Dec.	2017	8, 9, 30, 37, 38, 53, 65	31	24.2-29.6	7.9-40.6	A-D	5.2-18.4
Total		6-9, 30, 37, 38, 52-54, 65, 66	55	23.2-29.7	4.1-51.0	A-D	5.2-20.6

いては、成熟雌・雄個体および卵黄囊期仔魚の採集によって、河川感潮域上端で産卵すると推測されているに過ぎない（水谷ほか，2000；日比野ほか，2002a；水谷・松井，2006）。

本科他種をみると、アリアケヒメシラウオは淡水性が強い感潮域上部に（田北，1966），シラウオは汽水域に（千田，1973a, b），有明海には分布しないイシカワシラウオ *Salangichthys ishikawae* Wakiya and Takahashi, 1913（細谷，2013）は外海に面する沿岸に（SENTA *et al.*, 1986；宮内・千田，1989），それぞれ主に分布し、通し回遊は行わない。松井・水谷（2001）で示唆されているように、アリアケシラウオが遡河回遊魚ならば、本種のみが特異な生活史をもつことになる。

近年、明らかに激減した絶滅危惧種であるアリアケシラウオの保全は緊急の課題であり、その解決には再生産の過程を明らかにすることが極めて重要である。本報告では、採集時の詳細な物理環境と共に、本種の産卵場について再検討した。

2. 材料と方法

仔稚魚調査は2014年から2017年の4年間（Table 1），秋季（11もしくは12月）の大潮前後に、有明海湾奥部に設けた32定点（2017年）から35定点（2015年）（Fig. 1）で行った。浮遊個体を採集するために稚魚ネット（口径1.3 m，網目0.5 mm）による近底層から表層までの傾斜曳を行ったが、その中で、懸濁物の多い河川感潮域（Stns. 0-5, 33-36, 50-53）では目詰まりを軽減するため

網目を1 mmとした。仔稚魚の密度（ $n \cdot 100 \text{ m}^{-2}$ ）は、網口に装着した濾水計（General Oceanics, 2030R）の回転数から求めた濾水量（ V, m^3 ）とメモリー深度計（Alec Electronics, Mark5）による最大水深（ d, m ）から $[n \cdot d \cdot V^{-1} \cdot 100]$ の式によって求めた。底生個体は、桁網 [KUIPERS (1975) を改変: 網口幅 (1.5 m)，高さ (0.25 m)，網目 (2 mm)] によって採集した。その仔稚魚の密度（ $n \cdot 100 \text{ m}^{-2}$ ）はGPS（Garmin, Colorado 300）で計測した曳網距離（ m ）に網口幅を乗じた曳網面積（ A, m^2 ）を算出して、 $[n \cdot A^{-1} \cdot 100]$ によって求めた。

各採集物は船上にて10%ホルマリン溶液で固定し、直ちに実験室に持ち帰り、選別後80%エタノール液で保存した。試料は、発育段階（KENDALL *et al.*, 1984）毎に、体長（BL）[屈曲期以前で脊索長（NL），後屈曲期以降で標準体長（SL）]，体高（胸鰭基底，BD）および最大卵黄高（ymh）（Fig. 3を見よ）を計測した。

物理環境は全ての定点において、水温（ $^{\circ}\text{C}$ ），塩分，濁度（NTU）をCompact-STD（JFEアレック，ASTD687）で表層から，流向・流速（ kt ）をADCP（RD Instruments, WHSZ-1200-I-UG12）で水深1 mから，それぞれ水底までを0.5 m間隔で，各定点で停船して計測した。観測線（Axis）をStn. 63を起点として，それぞれ諫早湾（Axis-1），塩田川（Axis-2），六角川（Axis-3），早津江川（Axis-4）および沖端川（Axis-5）まで設けた（Fig. 1）。

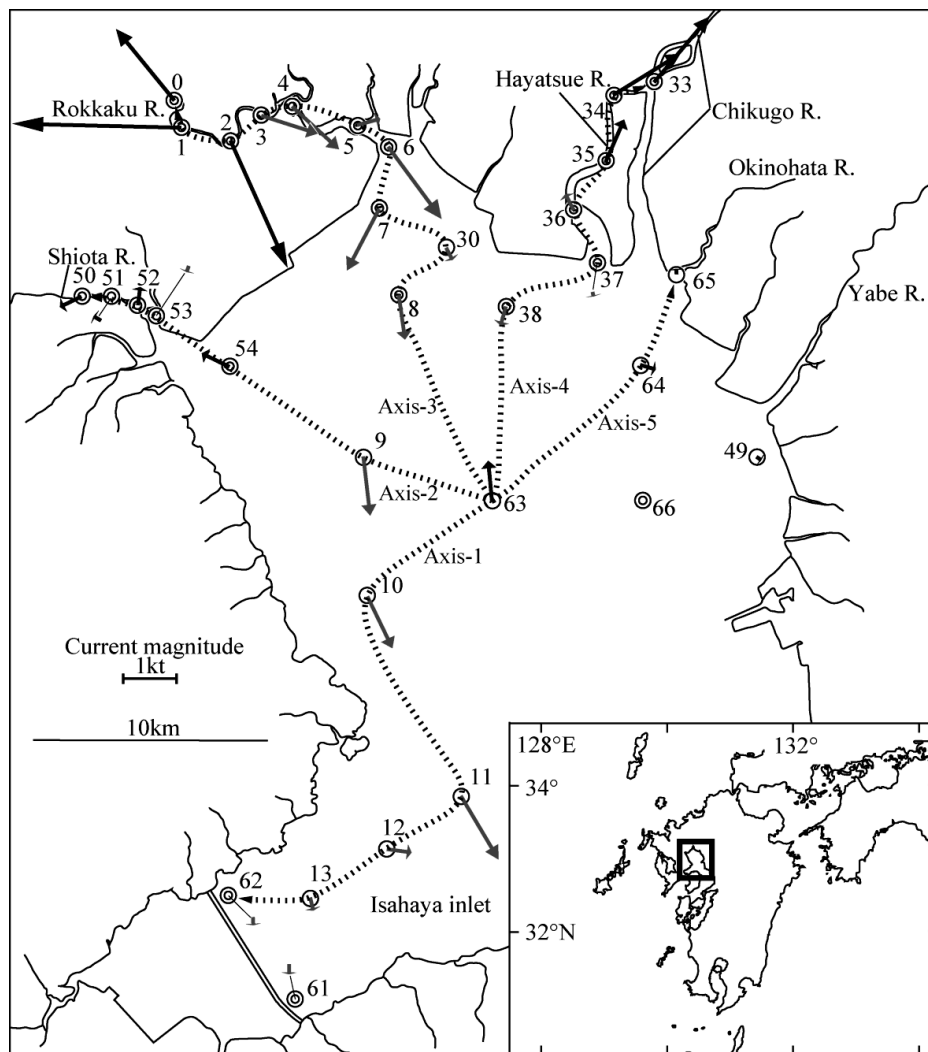


Fig. 1 Chart of Ariake Bay showing the stations where fish larvae and juveniles were surveyed in November 2014 and 2015, and December 2016 and 2017. Pelagic fishes were collected by oblique tows from near the bottom to surface with a larva net at all *circle* stations, of which, *double circles* were the stations at which demersal fishes were collected also by a beam trawl. *Solid* (flood tide) and *shade* (ebb tide) *arrows* show tidal direction and magnitude (kt) at 1 m depth of each station, when larvae and juveniles were collected in 2017. Five dotted axes extended from a core station (Stn. 63) to each area are to observe profiles of water parameters.

2014 から 2017 年の 4 年間で、アリアケシラウオの卵黄囊期仔魚から後屈曲期仔魚、合計 55 尾 (5.2-20.6 mm BL) が採集された (Table 1)。本報告は、最も多く採集された主に 2017 年の試料に

基づいて記述した。

本研究で用いた仔魚は、筋節数が 70 以上、尾柄部背面に黒色素胞がなく、臀鰭基底起部は背鰭第 6 軟条直下であったことからアリアケシラウオと

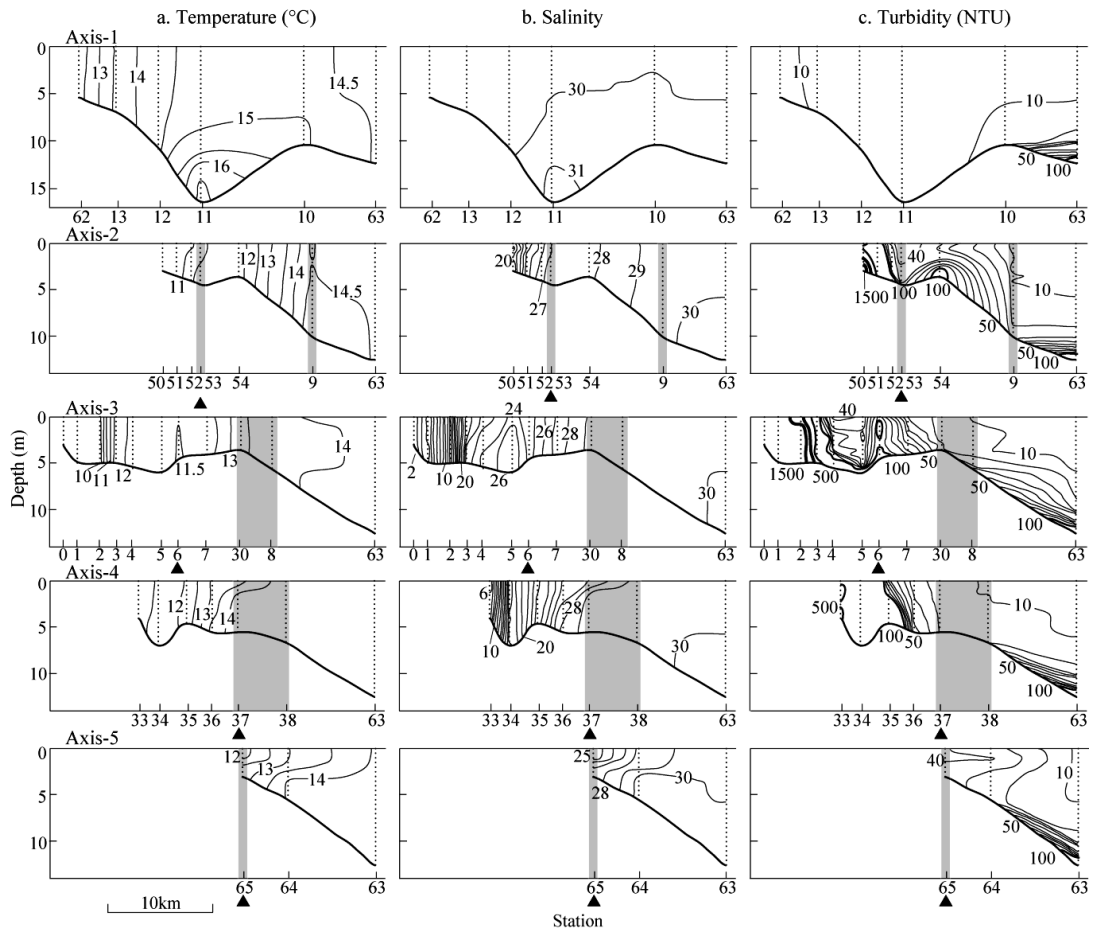


Fig. 2 Vertical and horizontal profiles of water parameters along each axis (see Fig. 1) in December 2017. Triangles under horizontal axes indicate river mouths. Shade areas indicate waters in which *Salanx ariakensis* larvae were collected with a larva net.

同定した (WAKIYA and TAKAHASHI, 1937; 水谷ほか, 2000; 日比野ほか, 2002a)。形態記載に用いた個体は、高知大学海洋生物研究教育施設に UKU 161000-161003 として登録した。

3. 結果

3.1 物理環境

2017年12月、主に上げ潮時での河川内では、六角川での最速3.2 kt、早津江川での最速1.6 ktの比較的速い潮流が、塩田川では0.5 kt以下と比較的遅い潮流がそれぞれ観測された。一方、主に下げ潮時の河口から沿岸域では、六角川沖の

Axis-3からAxis-1のものが0.8-1.6 ktと卓越し、諫早湾では著しく遅い潮流であった (Fig. 1)。水温および塩分でみると、塩田川、六角川および早津江川では河口から上流にかけての水塊は強混合状の高濁度水塊であった (Fig. 2 (a, b))。河川内では、著しく変化した塩分は、河口から湾奥部にかけては、緩やかに30前後まで増加した (Fig. 2 (b))。濁度 (NTU) は、六角川および塩田川の1900以上、早津江川の500以上と著しく高かったが、河口から沖合もしくは諫早湾にかけて徐々に減退し、10以下になっていた (Fig. 2 (c))。

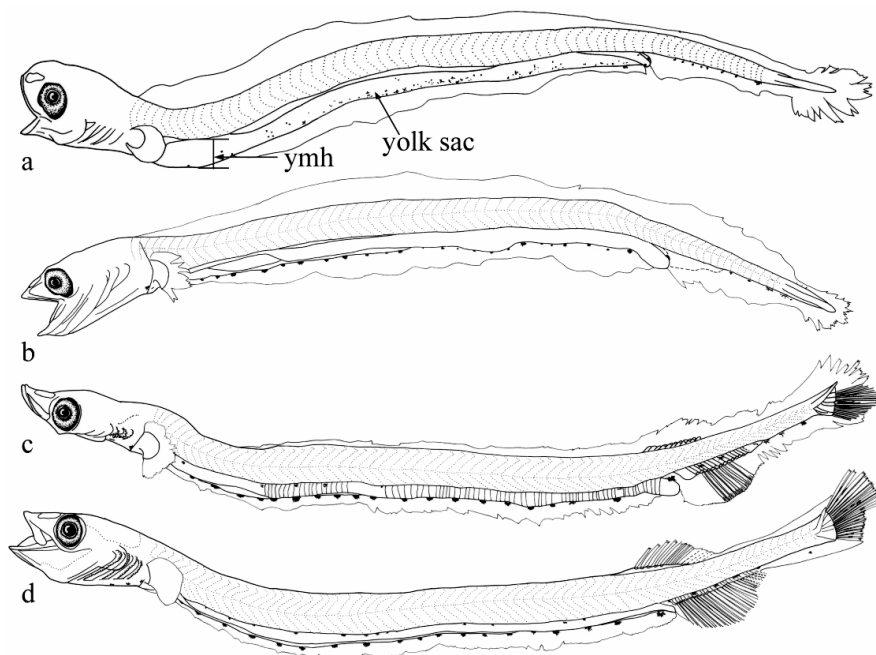


Fig. 3 Developmental stages of *Salanx ariakensis* collected in the present study. a, 5.3 mm yolk-sac larva (UKU-161000); b, 8.3 mm preflexion larva (UKU-161001); c, 14.0 mm flexion larva (UKU-161002); d, 18.4 mm postflexion larva (UKU-161003). ymh = yolk sac maximum height.

3.2 仔魚の形態 (Figs. 3, 4)

2017年12月に採集された仔魚は、体長（以下略）5.2–18.4 mmの卵黄囊期仔魚から後屈曲期仔魚であり（Table 1, Fig. 3），その中でも，卵黄囊期と前屈曲期（5.2–12.8 mm）の仔魚が，全体のおよそ2/3を占めた（Fig. 4）。

日比野ほか（2002a）は，本種の天然仔魚に関して詳細な形態記載を行っているが，卵黄に関してほとんど触れていなかった。そこで本報告では卵黄の推移を中心に個体発生を記載する。筋節数は，各发育段階を通して $52-55 + 16-21 = 70-74$ であった（Fig. 3）。6 mm 未満の個体では，眼は黒化，口および肛門は開口していた。卵黄は直腸まで達しており，約6 mmで完全に消滅するまで，最後まで体軸とは垂直の方向に吸収され，卵黄囊の高さは低くなっていった（Fig. 3 (a)）。最大卵黄高/体高は，約5 mmで約50%であったが，約6 mmで0%になっていた。卵黄吸収後，

脊索尾端の上屈は約13 mmで始まり，約16 mmで完了し，尾鳍主鳍条もほぼ完成していた。臀・背鳍の基底は，前屈曲期中・屈曲期中にそれぞれ分化し始め，鳍条は，臀鳍では屈曲期中に分化し始めたが，背鳍では全く分化しておらず，背・臀鳍の発達は非同時的であった。その後，後屈曲期においても，両鳍の鳍条は後半部を残し未完成であった。

顕著な黒色素胞について述べると，卵黄には，その腹縁正中線を中心に微小な黒色素胞が散在していた。卵黄吸収に伴い，これらの色素は消失していったが，腹縁膜縁に20–25個の比較的大きな点状の色素が胸部から直腸に渡って一列をなしていた。この色素列は，发育に伴う膜縁の退縮によって腸下縁へと移動していた。尾柄部背縁の黒色素胞は，全发育段階を通して出現していなかった（Fig. 3 (a-d)）。

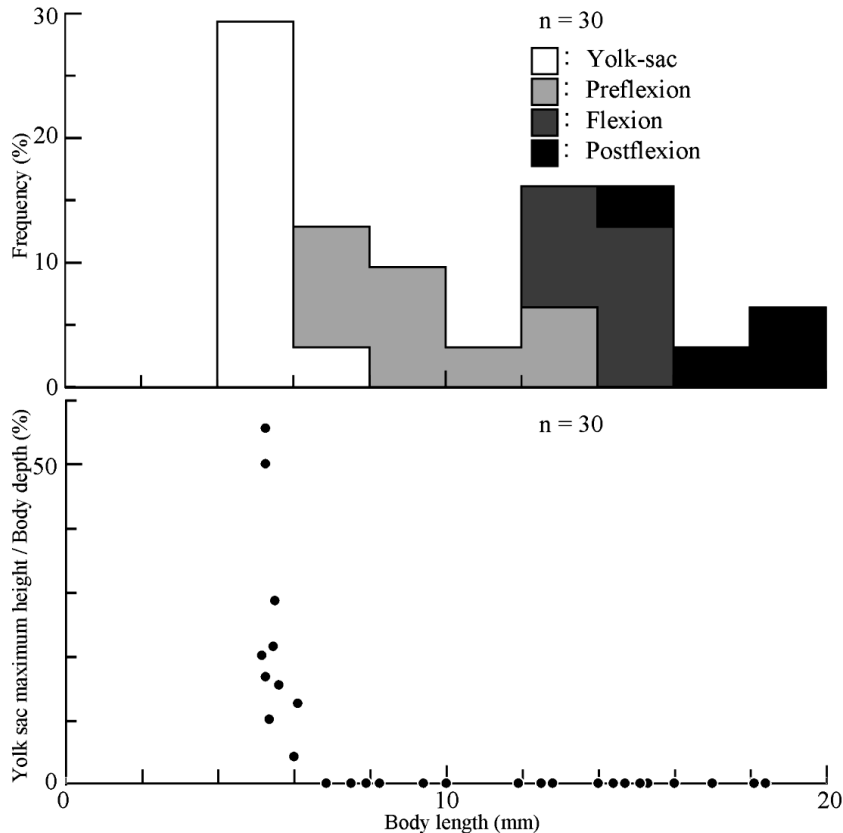


Fig. 4 Size frequency distribution for developmental stages (top) and absorption process of yolk with growth (bottom) in *Salanx ariakensis* larvae (yolk sac maximum height: see Fig. 3).

3.3 仔魚の分布

2017年12月の調査では、仔魚は、稚魚ネットによってのみ採集され、桁網ではいずれの定点でも全く採集されなかった。仔魚は河口付近 (Stns. 30, 37, 53, 65) および湾奥部 (Stns. 8, 9, 38) で出現し、河川内 (Stns. 0-7, 33-36, 50-52) および諫早湾 (Stns. 11-13, 61, 62) では、出現しなかった (Fig. 5)。发育段階別にみると、卵黄囊期仔魚 (5.2-6.1 mm) は、早津江川と沖端川の河口周辺 (Stns. 30, 37, 65) および早津江川の滞筋 (Stn. 38) で出現した一方、後屈曲期仔魚 (16.0-18.4 mm) は、湾奥部 (Stn. 9)、早津江川の滞筋 (Stn. 38) および塩田川河口 (Stn. 53) で出現した (Fig. 5)。これらを各観測線 (Axis) の物理環境の水平分布

と照らし合わせると、仔魚は、おおよそ水温 11-14℃、塩分 24-30、濁度 8-60 の範囲で出現し、有明海湾奥部には比較的高鹹で低濁度の水塊に分布していた (Fig. 2)。

一方、2014-2016年では、本種仔魚は2017年と同様に河口周辺の水域での稚魚ネットの傾斜曳によって採集され、河川感潮域および桁網では全く採取されなかった (Table 1)。特に、卵黄囊期仔魚および前屈曲期仔魚をみると、2014年では早津江川河口周辺で、2015年では塩田川河口域で、2016年では矢部川の河口沖で出現した。仔魚の出現した定点の表層の物理環境は、おおよそ塩分 23-30、濁度 4-51 の範囲であり、これら3ヶ年の傾向は2017年のものとほぼ一致した。

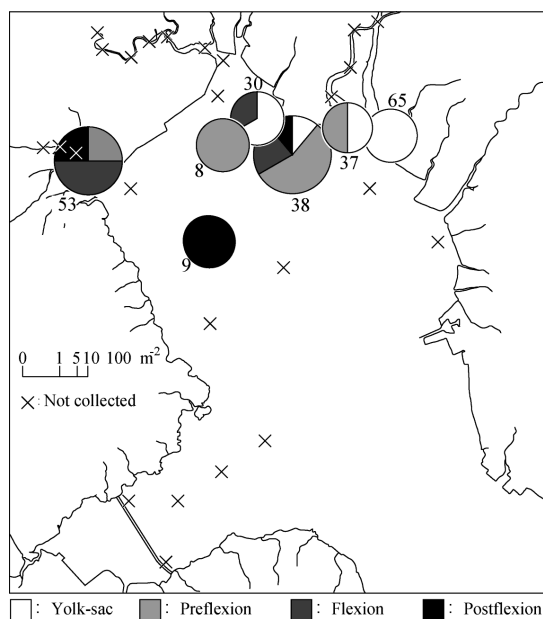


Fig. 5 Horizontal distribution of *Salanx ariakensis* larvae collected by a larva net in Ariake Bay, December 2017. The diameter of each circle is drawn in proportion to the square root of density ($n \cdot 100 \text{ m}^{-2}$), of which the largest was 24 at Stn. 38. Numeral beside each circle shows station number (see Fig. 1).

4. 考察

本種の肛門直前まで達する細長い卵黄は、本科他種の仔魚にもみられるが (OKADA and MORI, 1958; 田北, 1966), 本種と同じキュウリウオ亜目 Osmeroidei に属するキュウリウオ科 Osmeridae とアユ科 Plecoglossidae (NELSON *et al.*, 2016) の卵黄は、躯幹部前半部までの一般的なものであり (疋田, 1958; 内田, 1958; YAMADA, 1963; YANAGAWA, 1978; TACHIHARA and KAWAGUCHI, 2003), 本種の卵黄はキュウリウオ亜目中、シラウオ科特有の形質であると言える。ちなみに、長大な卵黄はコイ科 Cyprinidae では普遍的な形質である (宮地ほか, 1963; SAKAI, 1990)。

この特異な卵黄から、内部栄養期を長時間過ごすと思われすが、本種の卵黄は、体長 5–6 mm という狭い範囲で吸収され、極めて短期間の成長

で消費されていると推測される。飼育された個体では、孵化後遅くとも 2 日までは、この長大な卵黄は残っている (水谷ほか, 2000)。しかし、この孵化後 2 日目の個体では、腹縁の色素列は既に腸に移っており、我々の卵黄囊期仔魚 (Fig. 3 (a)) と比較して、明らかに色素の発達がより進んでおり、孵化直後の仔魚の色素分布などについては、今後、検討するべきである。この卵黄吸収の時間的経過は天然仔魚の耳石輪紋を用いて明らかにする必要がある。

本研究では、河川内からアリアケシラウオ仔魚は採集されず、仔魚が出現した定点の物理環境は比較的、高鹹かつ低濁度を示し、卵黄囊期仔魚は、早津江川と沖端川の河口周辺に集中していた (Figs. 2, 5)。水谷ほか (2000) および日比野ほか (2002a) は、本研究の筑後川での最上流の定点 (Stn. 33) から約 7 km 上流で、本種の一対の雌雄成熟個体および卵黄囊期個体をそれぞれ採取し、両者とも本種の産卵場は河川感潮域上端と推測している。日比野ほか (2002a) での早期仔魚を採取した定点と水谷ほか (2000) での親魚を採取した定点は、ほぼ同水域と考えられ、そこでの塩分は常に 0 ではなく、潮汐によっては 0.1–0.5 を示すこともある (日比野ほか, 1999; 平井, 2002)。また、我々の Stn. 33 の 2017 年 12 月における塩分は 6 以下であったが、潮汐によって、ほぼ 0 になることも珍しくない (SIMANJUNTAK, 2016)。すなわち、前・後者の調査点は、距離的には離れているが、同じ感潮域に含まれ、前者の感潮域最上端付近のみが産卵場であるとは考えがたい。

本研究では、稚魚ネットの傾斜曳によって、仔稚魚を近底層から表層まで把握した。仮に、河川外で本種の卵黄囊期仔魚が中層から近底層に分布するならば、稚魚ネットの表層曳によって調査した日比野ほか (2002a) は、これらを見逃していた可能性がある。日比野ほか (2002a) も、同河口付近で卵黄囊期仔魚を採取している。

河口付近で産卵・孵化する特産種の本種 *Acanthogobius hasta* (内田, 1936) の卵黄囊期仔魚の一部は上げ潮によって塩分 0 に近い河川感潮域上部にまで達することを考慮すると (異儀田,

1986; 東島ほか, 未発表), 本種の卵黄嚢期仔魚および成魚も, 1.5 kt を超える (Fig. 1) 上げ潮によって, 河川感潮域上部まで運ばれる可能性を否定できない。

成魚の詳細な知見は乏しい中, 成熟雌は, 河口周辺で頻繁に出現し (小早川みどり, 私信), 本種を対象とした漁業は, 筑後川や沖端川の河口域を中心に行われていた (松井, 1995)。一方, 採集状況など不明確ではあるが, 本種の卵および仔魚が河川感潮域で採取されている事例もある (水谷・松井, 2006)。

本科他種をみると, アリアケヒメシラウオは河川感潮域に留まり, シラウオは河口周辺の汽水域, およびイシカワシラウオは沿岸浅海域で, それぞれ産卵する (田北, 1966; 千田, 1973a, b; 宮内・千田, 1989)。したがって, このことから考えると, 本種のみを遡河回遊は特異と言える。

以上, これらの事実を鑑みて, 本種もシラウオと同様に河口周辺の汽水域で産卵する可能性が高い。また, 卵黄吸収後, 仔魚は発育に伴い西方面に反時計回りの恒流 (井上, 1980) によって分散し成育していることが窺え (Fig. 5), 湾奥部の沿岸域を成育場としていることが推測される。

底生魚の採集に用いた網目 2 mm の桁網には, アリアケシラウオ仔魚は 4 年間の全定点で皆無であった。この網目では, 仮に早期仔魚が底生であった場合, ほとんどの個体がそれを通過したことは否めない。しかし, 本桁網では, 体長 20 mm 以下のコイチ *Nibea albiflora*, ハゼクチ, ワラスボ *Odontamblyopus lacepedii*, ショウキハゼ *Tridentiger barbatus*, デンベエシタビラメ *Cynoglossus lighti*, 体長 25 mm 前後のエツ *Coilia nasus* などの着底間もない底生稚魚が採集されており (青山ほか, 2007; YAGI *et al.*, 2011; SIMANJUNTAK, 2016; 伊藤ほか, 2018), 本種の稚魚から成魚期にかけて全く採取されなかったことは, アリアケシラウオは少なくとも稚魚期以降は底生生活を送らないことを示している。

これらの推測が正しいならば, 絶滅危惧種である本種の保護にとって, 再生産の場である湾奥の河口周辺および浅海域の保全は重要であろう。

謝 辞

研究の基地となった佐賀県有明水産振興センターの歴代の所長および職員の方々に厚くお礼申し上げます。有益な論議をして頂いた愛知県水産試験場漁業生産研究所の日比野学博士に深く感謝する。貴重な情報を頂いた福岡市在住の小早川みどり博士に深く御礼申し上げます。匿名の校閲者 2 名の方々には, 本稿を改善するにあたり有益な御助言を賜り, 心より感謝する。複雑な地形を有する有明海において適切な船頭をして下さった片瀬久人氏にお礼申し上げます。

引用文献

- 青山大輔・木下 泉・藤田真二 (2007): 有明海湾奥部河口域の魚類成育場としての役割: 特産種と普通種の違い. 有明海生態系 かけがえのない内湾: その特徴と異変からの回復をめざして-2 (東幹夫・木下 泉編), 海洋と生物, 29, 16-25.
- 日比野 学・上田拓史・田中 克 (1999): 筑後川河口域におけるカイアシ類群集とスズキ仔稚魚の摂餌. 日本水産学会誌, 65, 1062-1068.
- 日比野 学・木下 泉・太田太郎・田中 克 (2002a): 筑後川河口で採集されたアリアケシラウオ仔魚の形態. 魚類学雑誌, 49, 103-108.
- 日比野 学・太田太郎・木下 泉・田中 克 (2002b): 有明海湾奥部の干潟汀線域に出現する仔稚魚. 魚類学雑誌, 49, 109-120.
- 疋田豊治 (1958): 柳葉魚 (シヤマモ) *Spirinchus lanceolatus* (Hikita) の発生について. 水産孵化場研究報告, 13, 39-49.
- 平井慈恵 (2002): 浸透圧調節整理. スズキと生物多様性: 水産資源生物学の新展開 (田中 克・木下 泉編), 恒星社厚生閣, 東京, p. 103-111.
- 細谷和海 (2013): シラウオ科. 日本産魚類検索 全種の同定 第三版 (中坊徹次編), 東海大学出版会, 秦野, p. 361.
- 異儀田和弘 (1986): 六角川感潮域における稚仔魚等の分布について. 佐賀県有明水産試験場研究報告, 10, 35-45.
- 井上尚文 (1980): 有明海の物理環境. 月刊海洋科学, 12, 116-126.
- 伊藤毅史・C. P. H. SIMANJUNTAK・木下 泉・藤田真二 (2018): 有明海六角川におけるエツ仔稚魚の分布. 水産増殖, 66, 17-23.

- KENDALL, A. W. Jr., E. H. AHLSTROM and H. G. MOSER (1984): Early life history stages of fishes and their characters. In Ontogeny and systematics of fishes. MOSER, H. G., W. J. RICHARDS, D. M. COHEN, M. P. FAHAY, A. W. KENDALL Jr. and S. L. RICHARDSON (eds.), Am. Soc. Ichthyol. Herpetol., Spec. Publ. 1, Lawrence, p. 11-22.
- 小早川みどり (2015): アリアケシラウオ, アリアケヒメシラウオ. レッドデータブック 2014 日本の絶滅のおそれのある野生動物 4 汽水・淡水魚類 (環境省自然環境局野生生物課希少種保全推進室編), ぎょうせい, 東京, p. 54-57.
- KUIPERS, B. (1975): On the efficiency of a two-metre beam trawl for juvenile plaice (*Pleuronectes platessa*). Neth. J. Sea Res., 9, 69-85.
- 松井誠一 (1995): アリアケシラウオ. 日本の希少な野生水生生物に関する基礎資料 (II), 日本水産資源保護協会, 東京, p. 206-211.
- 松井誠一・水谷 宏 (2001): 日本産シラウオ類の幼型成熟と種分化. 月刊海洋, 33, 148-153.
- 宮地傳三郎・川那部浩哉・水野信彦 (1963): 原色日本淡水魚類図鑑. 保育社, 大阪, xii + 275 pp., pls. 1-44.
- 宮内康子・千田哲資 (1989): イシカワシラウオ. 山溪カラー名鑑 日本の淡水魚 (川那部浩哉・水野信彦編), 山と溪谷社, 東京, p. 53, 82-83.
- 水谷 宏・松井誠一 (2006): 有明海に固有な絶滅危惧種, アリアケシラウオとアリアケヒメシラウオの生態. 魚類環境生態学入門: 溪流から深海まで, 魚と棲みかのインターアクション (猿渡敏郎編), 東海大学出版会, 秦野, p. 134-152.
- 水谷 宏・松井誠一・竹下直彦 (2000): アリアケシラウオの卵内発生と仔稚魚の形態変化. 水産増殖, 48, 497-502.
- NELSON, J. S., T. C. GRANDE and M. V. H. WILSON (2016): Fishes of the world, 5th ed. John Wiley & Sons, Hoboken, xli + 707 pp.
- OKADA, Y. and K. MORI (1958): Ecological study of *Salangichthys microdon* in breeding season: II. Development of the "white fish", *Salangichthys microdon*. Rep. Fac. Fish. Pref. Univ. Mie, 3, 26-28, pls. 1-2.
- SAKAI, H. (1990): Larval developmental intervals in *Tribolodon hakonensis* (Cyprinidae). Jpn. J. Ichthyol., 37, 17-28.
- 千田哲資 (1973a): 岡山県高梁川におけるシラウオの産卵場. 魚類学雑誌, 20, 25-28.
- 千田哲資 (1973b): 岡山県高梁川における産卵期のシラウオ. 魚類学雑誌, 20, 29-35.
- SENTA, T., I. KINOSHITA and T. KITAMURA (1986): Larval ishikawa icefish, *Salangichthys ishikawae* from surf zones of central Honshu, Japan. Bull. Fac. Fish. Nagasaki Univ., 56, 29-34.
- SIMANJUNTAK, C. P. H. (2016): Early life history of the endemic engraulid, *Coilia nasus*, in Ariake Bay. Doctor Thesis, Kochi Univ., 153 pp.
- TACHIHIRA, K. and K. KAWAGUCHI (2003): Morphological development of eggs, larvae and juveniles of laboratory-reared Ryukyu-ayu *Plecoglossus altivelis ryukyuensis*. Fish. Sci., 69, 323-330.
- 田北 徹 (1966): アリアケヒメシラウオの生態, 生活史. 長崎大学水産学部研究報告, 20, 159-170.
- 内田恵太郎 (1936): ハゼクチの生活史. 動物学雑誌, 48, 182.
- 内田恵太郎 (1958): アユ *Plecoglossus altivelis* Temminck et Schlegel. 日本産魚類の稚魚期の研究第1集, 九州大学農学部水産学第二教室, 福岡, p. 18-20, pls. 18-20.
- WAKIYA, Y. and N. TAKAHASHI (1937): Study on fishes of the family Salangidae. J. Coll. Agr. Tokyo Imp. Univ., 14, 265-296.
- YAGI, Y., I. KINOSHITA S. FUJITA, D. AOYAMA and Y. KAWAMURA (2011): Importance of the upper estuary as a nursery ground for fishes in Ariake Bay, Japan. Environ. Biol. Fish., 91, 337-352.
- YAMADA, J. (1963): The normal developmental stages of the pond smelt, *Hypomesus olidus* (Pallas). Bull. Fac. Fish. Hokkaido Univ., 14, 121-126.
- YANAGAWA, H. (1978): Embryonic development and fry of the kyûriuo, *Osmerus eperlanus mordax* (Mitchill). Bull. Fac. Fish. Hokkaido Univ., 29, 195-198.

受付: 2019年10月7日

受理: 2019年11月8日

資 料

第 57 卷第 3・4 号掲載欧文論文の和文要旨

Khin Khin Gyi¹⁾, 大村 卓朗^{2, 3)}*, 中村 理絵³⁾, 田中 祐志^{1, 2)}: 粒子画像解析装置 FlowCAM を用いた植物プランクトンの高分解能観察

水柱の環境特性と関連した微細規模の時空間における植物プランクトン動態を理解するために、水中ポンプを用いて深さ 0.5-2 m 間隔で、一昼夜に亘り 4 時間毎に 6 回のサンプリングを行った。自動的に粒子形状識別とサイズ計測ができる FlowCAM が、植物プランクトンの分析に活用された。その結果、植物プランクトンは、鉛直的に数 m、時間的に数 h 以内で大きく変動した。例えば、*Thalassiosira* sp. と *Prorocentrum minimum* はすべてのサンプリング深度と時間で比較的均等に検出されたが、*Dactyliosolen fragilissimus* と *Scrippsiella trochoidea* の水柱総現存量は初め 2 回のサンプリングの後、有意に減少した。種毎にそれぞれ、鉛直分布は各サンプリング時刻の水温躍層の状態と関連していた。このような植物プランクトンの種特異的の分布および組成の変動は、植物プランクトンの生態生理学的特性およびサイズ構成、ならびに短期間の海洋環境変動を反映している。底層中のクロロフィル *a* の高い値は、植物プランクトンだけでなく凝集粒子の蛍光がもたらしたと考えられた。

(1 東京海洋大学 海洋科学技術研究科 〒108-8477 東京都港区港南 4-5-7, 2 東京海洋大学 海洋資源環境学部 〒108-8477 東京都港区港南 4-5-7, 3 (株)水圏科学コンサルタント 〒144-0031 東京都大田区東蒲田 2-30-17 サンユ-東蒲田ビル 5F, *連絡先著者: 大村 卓朗 (おおむらたくお) Tel : 03-6428-6715 Fax : 03-6428-6716 E-mail : omura@lasc.co.jp)

Nur Indah SEPTRIANI¹⁾ · Chinthaka Anushka HEWAVITHARANE¹⁾ · Bambang RETNOAJI²⁾ · 望岡典隆¹⁾* : インドネシア中部ジャワのセガラアナカンにおける *Anguilla bicolor bicolor* の銀化変態に伴う形態変化

Anguilla bicolor bicolor の銀化変態に伴う形態的变化を明らかにするため、2016 年~2018 年にインドネシア中部ジャワのチラチャップ市セガラアナカンで 69 個体の雄と 38 個体の雌を採集した。得られた標本は体色と胸びれの色彩によって、黄ウナギ期は 2 期に、銀ウナギ期は 3 期に区分された。本種の銀化開始サイズは雄では全長 342-501 mm, 414.8 ± 40.4 (平均 ± SD), 雌では全長 674-937 mm, 786.1 ± 69.0 であり、雄は 5 月と 6 月 (乾季) に、雌は周年採捕された。雌雄ともに、銀化の進行に伴い背鰭高、臀鰭高、尾鰭高、胸鰭長の全長比等の遊泳に関する指標は有意に大きくなった。摂餌に関する指標は、雄の上・下顎長の全長比は銀化の進行に伴って有意に大きくなり、その他の形質も顕著な変化は認められず、加えて、餌で誘引する漁具で採捕されていることから、本種では銀化変態中も摂餌していると考えられた。

(1 九州大学大学院農学研究院, 2 ガジャマダ大学, *連絡先著者住所: 〒819-0395 福岡県福岡市西区 744 九州大学大学院農学研究院 電話番号: 092-802-4603 ファックス番号: 092-802-4603 E-mail : mochioka@agr.kyushu-u.ac.jp)

学 会 記 事

1. 幹事会議事録

2019年度第2回幹事会議事録

日時：2019年9月6日（金）13時15分～13時40分

場所：東京海洋大学品川キャンパス 2号館200A

参加者：小松，今脇，高柳，小池，田中，荒川，奥村，柳本，本多（事務局）

(1) 報告事項

- ① 第1回水産・海洋科学研究連絡協議会（2019年5月30日，海洋大品川キャンパス）について荒川庶務幹事から報告があった。
- ② 2019年度総会，評議員会および学術研究発表会（2019年6月8日，日仏会館）について荒川庶務幹事から報告があった。
- ③ 第1回日仏関連学会連絡協議会（2019年6月20日，日仏会館）について荒川庶務幹事から報告があり，2020年度「日仏会館学術研究助成」の公募が開始され，締め切りは11月である。また，8月末に日仏会館・フランス国立研究所所長が坂井セシル氏からベルナル・トマン氏に交代したことを受け，日仏海洋学会名誉会長もベルナル氏に変更する。
- ④ 2019年6月の総会で決定した投稿規定（和文および英文）について，ホームページに掲載した。この投稿規定は，2019年6月以降に投稿された論文から対象とする。
- ⑤ 学会誌 La mer 第57巻1-2号を発送済みであること，3-4号の編集状況および2017年度日仏海洋学シンポジウム（ボルドー）のプロシーディングスについて荒川庶務幹事（吉田編集委員長代理）から報告された。
- ⑥ オンラインジャーナルの本タイトルは【La Mer】，キータイトルは【La Mer (Tokyo, 1963)】になった。
- ⑦ 日仏会館科学講座「カキをめぐる日仏交流：歴史，産業，文化」は，2020年3月14日（土）に日仏会館ホールで開催予定であることが，小池渉外幹事より報告された。

(2) 審議事項

- ① 『日仏会館フランス事務所』から『日仏会館・フランス国立日本研究所』に名称変更されたことから，2020年度総会で会則第12条を修正することにした。
- ② 学会ホームページのトップページで，2019年6月総会で和文および英文の投稿規定を改定したことを通知した上で，La mer（学会誌）のトップページに改定した投稿規定を掲載することとし，内田・柳本広報幹事に作業を依頼した。
- ③ 日仏会館科学講座「カキをめぐる日仏交流：歴史，産業，文化」について意見交換した。

2. 所属および住所変更

氏名	新しい所属先
許 敏	Key Laboratory of Marine Ecology & Environmental sciences Institute of Oceanology, Chinese Academy of Science
高橋 義文	福岡県福岡市西区元岡 744 WEST5-861 九州大学大学院 農学研究院 農業資源経済学部門

3. 寄贈図書

Techno-ocean News（テクノオーシャンネットワーク）；No.71-72

Ocean Newsletter（海洋政策研究財団）；No.453-462

Ocean Breeze（東京大学大気海洋研究所）；第31号-第32号

FRANEWS（水産総合研究センター）；No.59-60

農村工学通信；No.116-117

東京大学大気海洋研究所 メーユ通信；No.14

水産技術（国立研究開発法人水産研究・教育機構）；第11巻第2号

国立科学博物館研究報告 A 類（動物学）；第44巻第4号，第45巻第1号-第45巻第2号

東京大学大気海洋研究所 要覧・年報 2019

人と海洋の共生をめざして 150人のオピニオンIX（海洋政策研究所）

賛 助 会 員

株 式 会 社 イ ー エ ム エ ス	兵庫県神戸市中央区東川崎町 1-3-3 神戸ハーバーランドセンタービル 13 F
い で あ 株 式 会 社	東京都世田谷区駒沢 3-15-1
公益財団法人海洋生物環境研究所	東京都新宿区山吹町 347 藤和江戸川橋ビル 7 階
ケー・エンジニアリング株式会社	東京都台東区浅草橋 5-14-10
J F E アドバンテック株式会社	兵庫県西宮市高畑町 3-48
株 式 会 社 新 協	東京都文京区大塚 4-40-1
株 式 会 社 セ ア ・ プ ラ ス	神奈川県横浜市緑区十日市場町 822-10
株 式 会 社 独 立 総 合 研 究 所	東京都江東区

(※詳細はセキュリティのため非公開)

日仏海洋学会入会申込書

(正・学生会員)

申込日 年 月 日
年度より入会

私は日仏海洋学会会則に同意し、下記の通り入会を申し込みます。

フリガナ			
氏名			
ローマ字			
生年月日	年 月 日	会誌送り先 (自宅 / 勤務先)	
メールアドレス			
勤務先			
勤務先住所	〒		
自宅住所	〒		
TEL		FAX	
紹介会員名			

■会員種別および会費 (不課税)

正会員：8,000円

特別会員^(*)：6,000円

学生会員：4,000円

賛助会員：1口 10,000円以上

※年度初めに満65歳以上で学会事務局へ申告した者

■事業年度 4月1日～翌年3月末日

■備考

入会申込書送付先：〒150-0013 東京都渋谷区恵比寿3-9-25

(財)日仏会館内

日 仏 海 洋 学 会

郵便振替番号：00150-7-96503

日仏海洋学会入会申込書

(賛助会員)

申込日 年 月 日
年度より入会

日仏海洋学会会則に同意し、下記の通り入会を申し込みます。

フリガナ			
会社・機関名			
住所	〒		
TEL		ご担当者名	
FAX		所属	
口座数 (1口1万円より)	口座	メールアドレス	
紹介会員名		TEL	

■事業年度 4月1日～3月末日

■備考

入会申込書送付先：〒150-0013 東京都渋谷区恵比寿 3-9-25

(財) 日仏会館内

日 仏 海 洋 学 会

郵便振替番号：00150-7-96503